



Article

<https://doi.org/10.1038/s41591-022-02128-z>

Autologous T cell therapy for MAGE-A4⁺ solid cancers in HLA-A*02⁺ patients: a phase 1 trial

Received: 9 December 2021

A list of authors and their affiliations appears at the end of the paper

Accepted: 9 November 2022

Published online: 09 January 2023

Check for updates

Affinity-optimized T cell receptors can enhance the potency of adoptive T cell therapy. Afamitresgene autoleucel (afami-cel) is a human leukocyte antigen-restricted autologous T cell therapy targeting melanoma-associated antigen A4 (MAGE-A4), a cancer/testis antigen expressed at varying levels in multiple solid tumors. We conducted a multicenter, dose-escalation, phase 1 trial in patients with relapsed/refractory metastatic solid tumors expressing MAGE-A4, including synovial sarcoma (SS), ovarian cancer and head and neck cancer ([NCT03132922](#)). The primary endpoint was safety, and the secondary efficacy endpoints included overall response rate (ORR) and duration of response. All patients ($N = 38$, nine tumor types) experienced Grade ≥ 3 hematologic toxicities; 55% of patients (90% Grade ≤ 2) experienced cytokine release syndrome. ORR (all partial response) was 24% (9/38), 7/16 (44%) for SS and 2/22 (9%) for all other cancers. Median duration of response was 25.6 weeks (95% confidence interval (CI): 12.286, not reached) and 28.1 weeks (95% CI: 12.286, not reached) overall and for SS, respectively. Exploratory analyses showed that afami-cel infiltrates tumors, has an interferon- γ -driven mechanism of action and triggers adaptive immune responses. In addition, afami-cel has an acceptable benefit–risk profile, with early and durable responses, especially in patients with metastatic SS. Although the small trial size limits conclusions that can be drawn, the results warrant further testing in larger studies.

Melanoma-associated antigen A4 (MAGE-A4) is a member of the MAGE protein family of cancer/testis antigens, with expression in healthy tissue restricted to immune-privileged sites¹. MAGE-A4 is expressed in solid cancers, including synovial sarcoma (SS), myxoid/round cell liposarcoma (MRCLS), non-small-cell lung cancer (NSCLC), head and neck squamous cell carcinoma (HNSCC) and ovarian, urothelial, melanoma and gastroesophageal cancers^{1–5}. MAGE-A4 is intracellularly processed, resulting in peptide fragments that are co-presented with human leukocyte antigens (HLAs) on the cell surface, forming epitopes that are weakly recognized by low-affinity natural T cell receptors (TCRs). Although immune checkpoint inhibitors have exhibited good clinical activity in patients with some MAGE-A4⁺ solid tumors, such as melanoma, other tumors, such as SS, may not respond as well^{6,7}.

Afamitresgene autoleucel (afami-cel) is an autologous, specific peptide enhanced affinity receptor, T cell therapy transduced via

a lentiviral vector to express a high-affinity and specific TCR targeted against a MAGE-A4_{230–239} peptide, GVYDGREHTV, presented by HLA-A*02 (ref. [6](#)). This TCR has been shown to respond potently toward MAGE-A4 peptides presented on multiple common HLA-A2 alleles. Preclinical assessment demonstrated that afami-cel induces potent cytotoxic effects and effector cytokine release against multiple HLA-A*02/MAGE-A4 cancer cells⁸, supporting the first-in-human phase 1 trial of afami-cel ([NCT03132922](#)).

Results

Patients

HLA-A*02-eligible and MAGE-A4-eligible patients were enrolled from a multicenter, screening protocol study ([NCT02636855](#)). A total of 854 HLA-A*02-eligible patients proceeded to tumor MAGE-A4 testing; 225 were MAGE-A4⁺. This phase 1 trial used a 3 + 3 design, involving afami-cel

dose escalation across dose Groups 1–3 and an expansion group. Dose ranges (total transduced cell number) were 0.08×10^9 to 0.12×10^9 cells (Group 1), 0.5×10^9 to 1.2×10^9 cells (Group 2), 1.2×10^9 to 6.0×10^9 cells (Group 3) and 1.2×10^9 to 10×10^9 cells (expansion group). Group 1 received cyclophosphamide (600 mg/m²/day) lymphodepletion (LD) chemotherapy on days −7, −6 and −5 and fludarabine (30 mg/m²/day) on days −7, −6 and −5. Group 2 received cyclophosphamide (600 mg/m²/day) LD chemotherapy on days −7, −6 and −5 and fludarabine (30 mg/m²/day) on days −7, −6 and −5. Group 3 received cyclophosphamide (600 mg/m²/day) LD chemotherapy on days −7, −6 and −5 and fludarabine (30 mg/m²/day) on days −7, −6, −5 and −4. Most patients in the expansion group ($n = 22$) received cyclophosphamide (600 mg/m²/day) LD chemotherapy on days −7, −6, and −5 and fludarabine (30 mg/m²/day) on days −7, −6, −5 and −4. Seven patients in the expansion group received the higher cyclophosphamide (1,800 mg/m²/day) LD chemotherapy on days −3 and −2 and combined with fludarabine (30 mg/m²/day) on days −5, −4, −3 and −2. Dose-limiting toxicities (DLTs) were evaluated before each dose escalation, with doses progressively increased to 1.2×10^9 to 10.0×10^9 cells in the expansion group. Eligible patients could receive a second cell infusion after disease progression after confirmed response.

Eligibility criteria included age ≥ 18 years to ≤ 75 years; histologically confirmed cancer diagnosis; positivity for at least one HLA-A*02 inclusion allele; MAGE-A4 RNA or protein expression in one or more tumor samples; and measurable disease according to Response Evaluation Criteria in Solid Tumors (RECIST) version 1.1 before LD chemotherapy (see Methods for full inclusion criteria). The sample size was not pre-specified and was based on clinical judgment. Up to 30 patients (including patients accrued during the dose-escalation phase) were treated in the dose-expansion phase, and up to an additional ten patients were treated in a radiation sub-study. The study was not statistically powered to evaluate safety or efficacy, and data are descriptive, with no formal hypothesis testing planned. The primary endpoints were adverse events (AEs), including serious AEs; laboratory assessments, including chemistry, hematology and coagulation; incidence of DLTs; determination of optimally tolerated dose range; and persistence of MAGE-A4^{C1032T} and replication-competent lentivirus over time. Secondary endpoints were overall response rate (ORR) confirmed by RECIST version 1.1; best overall response (BOR); time to response (TTR); duration of response (DoR); duration of stable disease (SD); progression-free survival (PFS); overall survival (OS); and presence of any of the following long-term follow-up (LTFU) AEs: new malignancies; new incidence or exacerbation of a pre-existing neurologic disorder and/or prior rheumatologic or other autoimmune disorder; new incidence of a hematologic disorder; opportunistic and/or serious infections; unanticipated illness and/or hospitalization deemed related to gene-modified cell therapy; and/or persistence of MAGE-A4^{C1032T} and replication-competent lentivirus over time. The exploratory endpoints included correlation of persistence, phenotype and functionality of transduced (afami-cel) and non-transduced T cells in the peripheral blood and/or tumor in response to treatment and safety; determination of target antigen expression, genes related to antigen processing/presentation and cell surface co-stimulatory ligands; and evaluation of serum cytokines (IL-6). The following exploratory endpoints were not analyzed: evaluation of anti-tumor antibodies or candidate biomarkers from plasma-derived exosomes and cell-free DNA. Owing to the preliminary nature of the data collected before the data cutoff, limited correlative analyses were reported relating to treatment response and safety. Two patients received a second infusion; they were non-responders. Therefore, ORR was not evaluated for the second infusion.

Sixty-three patients were deemed eligible and were enrolled into the intent-to-treat (ITT) population; 60 patients underwent leukapheresis; and 38 patients were treated with afami-cel (modified ITT (mITT) population) (Fig. 1 and Extended Data Fig. 1). Baseline patient characteristics are presented in Table 1 and Supplementary Tables 1

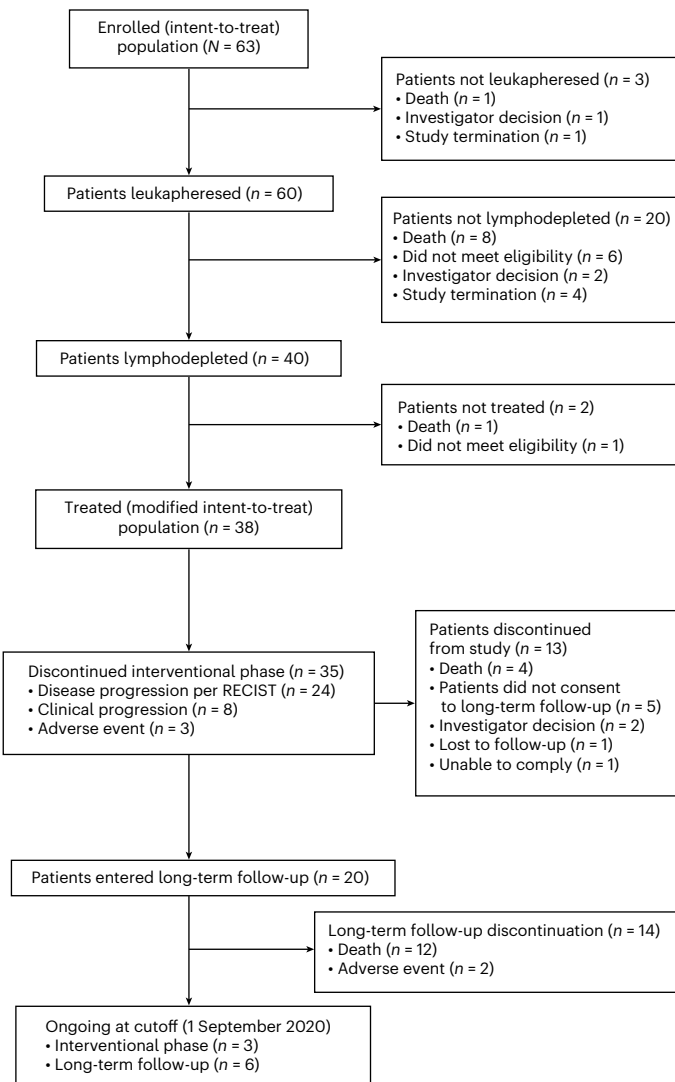


Fig. 1 | Study design and patient disposition. RECIST.

and 2. The first patient was enrolled on 5 July 2017; the last patient visit was 30 December 2019. Three patients did not undergo leukapheresis due to death, study termination and investigator decision (one each). Twenty patients underwent leukapheresis but did not receive LD chemotherapy or afami-cel due to death from disease under study (seven), death from unknown cause (one), not meeting eligibility criteria (six) or investigator decision (six). Two of the 40 patients who underwent LD chemotherapy did not receive afami-cel due to disease-related death or because they became ineligible after LD chemotherapy. The HLA-A2 and MAGE-A4 antigen scores in the mITT population are shown in Supplementary Table 1 and Extended Data Fig. 2. In the mITT population, three patients were treated in each dose-escalation group, and 29 patients were treated in the expansion group. The number (%) of patients with each indication are two (5.3) esophageal, one (2.6) gastric, three (7.9) head and neck, one (2.6) melanoma, two (5.3) NSCLC, nine (23.7) ovarian, two (5.3) urothelial, two (5.3) MRCLS and 16 (42.1) SS.

At baseline, 58% of the mITT patients were male, and their median age was 58 years (range, 31–78). The median number of prior lines of systemic therapy was three (range, 1–8), including neoadjuvant and adjuvant therapies (Table 1 and Supplementary Table 2). Among patients with SS (Supplementary Table 3), the median age was 49 years (range, 31–76), and the median number of prior lines of treatment was three (range, 1–6), including ifosfamide (100%), anthracyclines (81%) and pazopanib (31%). MAGE-A4 expression was heterogeneous within

Table 1 | Summary of patient characteristics (mITT population, N=38)

Parameter	Category	Statistic	Overall (N=38)
Age (years)		N	38
		Mean (standard deviation)	56.4 (12.59)
		Median	58.0
		Min, max	31, 78
Age categorization	<65 years	n (%)	28 (73.7)
	≥65 years	n (%)	10 (26.3)
Sex	Male	n (%)	22 (57.9)
	Female	n (%)	16 (42.1)
Ethnicity	Hispanic/Latino	n (%)	2 (5.3)
	Not Hispanic/Latino	n (%)	36 (94.7)
Race	White	n (%)	35 (92.1)
	Asian	n (%)	3 (7.9)
Primary tumor type	Esophageal	n (%)	2 (5.3)
	Gastric	n (%)	1 (2.6)
	Head and neck	n (%)	3 (7.9)
	Melanoma	n (%)	1 (2.6)
	NSCLC	n (%)	2 (5.3)
	Ovarian	n (%)	9 (23.7)
	Urothelial	n (%)	2 (5.3)
	MRCLS	n (%)	2 (5.3)
	SS	n (%)	16 (42.1)
ECOG score	0	n (%)	13 (34.2)
	1	n (%)	25 (65.8)
Time from initial diagnosis to T cell infusion (months) ^a		Mean (standard deviation)	51.4 (40.33)
		Median	40.4
		Min, max	7.3, 205.5
Prior lines of systemic therapy		Mean (standard deviation)	3.2 (1.88)
		Median	3.0
		Min, max	1, 8
Total transduced cells (×10 ⁹)		Mean (standard deviation)	6.1213 (3.422688)
		Median	6.4022
		Min, max	0.1, 9.9756

^aTime from initial diagnosis to T cell infusion in months was calculated as: (T cell infusion date – date since initial diagnosis + 1) × (12/365.25). max, maximum; min, minimum; N, total number of patients; n, number of patients.

individual tumor types and across the nine solid tumor types evaluated. The median MAGE-A4 histoscore (H-score) was 189 (range, 15–300) across all patients and 249 (range, 60–300) in patients with SS.

Twenty-one patients received cytotoxic bridging chemotherapy (Supplementary Table 2). Twenty patients (53%) entered LTFU: 12 (32%) died of disease progression; two (5%) discontinued owing to AEs; and six (16%) remain in LTFU. Of the 18 patients who did not enter LTFU, three were being followed at the data cutoff; 13 left during the interventional phase; and two completed the interventional phase but did not enter LTFU.

Safety

Toxicities determined by the Safety Review Committee as DLTs occurred in six patients and included cytopenias (four), aplastic anemia (one) and cerebrovascular accident (one); all DLTs occurred in the expansion group (median dose, 7.85×10^9 transduced cells) after dose escalation completion. All 38 patients in the mITT group had Grade ≥3 treatment-emergent AEs (TEAEs) (Table 2); hematologic toxicities were the most common, including Grade ≥3 decreased counts for lymphocytes (97%), neutrophils (87%) and platelets (42%) and anemia (63%). Grade ≥3 febrile neutropenia and pancytopenia occurred in 32% and 11% of patients, respectively. Prolonged cytopenia, defined as Grade ≥3 neutropenia, anemia or thrombocytopenia persisting at week 4 after afami-cel treatment, occurred in 17 patients (45%), including nine (24%) with prolonged neutropenia. Serious treatment-related systemic infections were infrequent (3%).

Duration/dose increases of the fludarabine and cyclophosphamide components of LD chemotherapy were made per the absence of DLTs. An additional day of fludarabine 30 mg/m² dosing was incorporated on day –4 for Group 3 (cyclophosphamide 1,800 mg/m²/day on days –3 and –2 and fludarabine 30 mg/m²/day on days –5, –4, –3 and –2). Because no hematological DLTs occurred in Group 3, the LD regimen was increased in the expansion group to a higher total dose of cyclophosphamide (3,600 mg/m² administered as 1,800 mg/m² on days –3 and –2), combined with four consecutive days of 30 mg/m² fludarabine. This was deemed scientifically justifiable because high-dose cyclophosphamide LD chemotherapy has been shown to support increased efficacy⁹.

Eighteen deaths were reported due to disease progression (14), AEs (three, two possibly treatment-related AEs) or comorbidities (one). Both treatment-related deaths were among the seven patients in the expansion group who received the highest LD dose regimen. The first was a 77-year-old patient with SS, heavily pre-treated with chemotherapy, who died of aplastic anemia on day 55 of the study. Grade 3 cytopenia developed in this patient from day –5 (LD chemotherapy day 3) and worsened after afami-cel infusion. Bone marrow biopsy on day 38 did not detect myelodysplastic syndrome, cytomegalovirus infection, enrichment of transduced T cells or MAGE-A4 antigen. The second was a 71-year-old patient with ovarian cancer who died of an ischemic cerebrovascular accident on day 17 after a Grade 3 neurotoxicity. Because of these two treatment-related fatalities, the maximum age at screening was reduced to 75 years, and the high-dose cyclophosphamide LD regimen was discontinued. The subsequent 22 patients in the expansion group reverted to the lower cyclophosphamide regimen.

Twenty-one patients (55%) had cytokine release syndrome (CRS)—ten (58%) Grade 1, nine (24%) Grade 2, one (3%) Grade 3 and one (3%) Grade 4; all events resolved (Supplementary Table 4). CRS occurred across all tumor types, with median time to onset of 3 days (range, 1–9) and median duration of 4 days (range, 1–19). Nine of the 19 patients (47%) with Grade 1 or 2 CRS were managed with supportive care. All Grade ≥3 CRS events were in patients with SS, including the patient in the expansion group who died of aplastic anemia.

Two patients (5%) had treatment-emergent, low-grade, early-onset, immune effector cell-associated neurotoxicity syndrome (ICANS)/encephalopathy, which was reversible and lasted 3 days or less: Grade 1 ICANS on day 3 in a patient with NSCLC with known brain metastasis and Grade 2 encephalopathy on day 8 in a patient with ovarian cancer without baseline brain metastasis. Six additional patients had other possible treatment-related neurological AEs, including tremor or headache. Nine expansion group patients had skin rashes possibly related to afami-cel, including three with Grade 3 severity. Skin rashes were typically reversible with supportive care and/or topical corticosteroids. Two patients with SS received a second afami-cel infusion after progressing from partial responses (PRs) achieved with the first afami-cel treatment. No new clinically important TEAEs developed after administration of a second round of LD chemotherapy followed by a second afami-cel infusion compared with their first LD

Table 2 | Incidence of TEAEs

Preferred term, n (%)	Group 1 (n=3)		Group 2 (n=3)		Group 3 + expansion group (n=32)		Overall (N=38)	
	All grades	Grade \geq 3	All grades	Grade \geq 3	All grades	Grade \geq 3	All grades	Grade \geq 3
Patients with any TEAEs	3 (100)	3 (100)	3 (100)	3 (100)	32 (100)	32 (100)	38 (100)	38 (100)
Lymphocyte count decreased	3 (100)	3 (100)	3 (100)	3 (100)	31 (96.9)	31 (96.9)	37 (97.4)	37 (97.4)
White blood cell count decreased	3 (100)	3 (100)	3 (100)	3 (100)	28 (87.5)	28 (87.5)	34 (89.5)	34 (89.5)
Neutrophil count decreased	3 (100)	3 (100)	3 (100)	3 (100)	27 (84.4)	27 (84.4)	33 (86.8)	33 (86.8)
Anemia	2 (66.7)	2 (66.7)	2 (66.7)	2 (66.7)	23 (71.9)	20 (62.5)	27 (71.1)	24 (63.2)
Fatigue	3 (100)	0	2 (66.7)	0	19 (59.4)	1 (3.1)	24 (63.2)	1 (2.6)
Nausea	3 (100)	0	2 (66.7)	0	19 (59.4)	0	24 (63.2)	0
Pyrexia	1 (33.3)	0	3 (100)	0	18 (56.3)	0	22 (57.9)	0
CRS	1 (33.3)	0	0	0	20 (62.5)	2 (6.3)	21 (55.3)	2 (5.3)
Platelet count decreased	2 (66.7)	1 (33.3)	1 (33.3)	1 (33.3)	18 (56.3)	14 (43.8)	21 (55.3)	16 (42.1)
Vomiting	2 (66.7)	0	2 (66.7)	0	15 (46.9)	1 (3.1)	19 (50.0)	1 (2.6)
Decreased appetite	3 (100)	0	2 (66.7)	0	11 (34.4)	2 (6.3)	16 (42.1)	2 (5.3)
Dyspnea	2 (66.7)	0	2 (66.7)	0	12 (37.5)	1 (3.1)	16 (42.1)	1 (2.6)
Hypophosphatemia	0	0	2 (66.7)	2 (66.7)	13 (40.6)	11 (34.4)	15 (39.5)	13 (34.2)
Diarrhea	2 (66.7)	0	0	0	12 (37.5)	0	14 (36.8)	0
Hypotension	0	0	1 (33.3)	1 (33.3)	13 (40.6)	3 (9.4)	14 (3.8)	4 (10.5)
Febrile neutropenia	1 (33.3)	1 (33.3)	2 (66.7)	2 (66.7)	9 (28.1)	9 (28.1)	12 (31.6)	12 (31.6)
Hyponatremia	2 (66.7)	2 (66.7)	1 (33.3)	0	9 (28.1)	6 (18.8)	12 (31.6)	8 (21.1)
Abdominal pain	2 (66.7)	0	2 (66.7)	0	7 (21.9)	1 (3.1)	11 (28.9)	1 (2.6)
Headache	0	0	3 (100)	0	7 (21.9)	0	10 (26.3)	0
Arthralgia	0	0	1 (33.3)	0	8 (25.0)	1 (3.1)	9 (23.7)	1 (2.6)
Aspartate aminotransferase increased	0	0	1 (33.3)	0	8 (25.0)	1 (3.1)	9 (23.7)	1 (2.6)
Chills	0	0	1 (33.3)	0	8 (25.0)	0	9 (23.7)	0
Dizziness	1 (33.3)	0	2 (66.7)	0	6 (18.8)	0	9 (23.7)	0
Alanine aminotransferase increased	0	0	1 (33.3)	0	7 (21.9)	1 (3.1)	8 (21.1)	1 (2.6)
Alopecia	1 (33.3)	0	2 (66.7)	0	5 (15.6)	0	8 (21.1)	0
Pruritus	0	0	1 (33.3)	0	7 (21.9)	0	8 (21.1)	0
Tumor pain	0	0	0	0	8 (25.0)	1 (3.1)	8 (21.1)	1 (2.6)

chemotherapy/afami-cel infusion schedules (Supplementary Table 5). Replication-competent lentivirus was not detected in any patient. Based on safety findings, the recommended phase 2 dose of afami-cel was 1.0×10^9 to 10×10^9 transduced cells.

Clinical activity

In the mITT population, ORR was 24% (95% confidence interval (CI): 11.4, 40.2; 9/38 patients) (Fig. 2a and Extended Data Fig. 3a). All nine patients with BOR of PR were treated in the Group 3/expansion cohort (highest T cell infusion group—seven SS, one HNSCC and one NSCLC of squamous histology) (Supplementary Table 6). The change in sum of longest diameter (SLD) of target lesions over time is shown in Fig. 2b. All responders had tumor MAGE-A4 H-scores of >200 , except one with HNSCC. The disease control rate (DCR) (percentage of patients with objective response or SD) was 74% (nine PR and 19 SD), including five of six patients with ovarian cancer in Groups 1 and 2. The median TTR was 6.4 weeks (95% CI: 6.1, 24.1), and median DoR was 25.6 weeks (95% CI: 12.3, not reached). The median PFS was 12.3 weeks (95% CI: 10.9, 19.1), and median OS was 42.9 weeks (95% CI: 20.7, not reached) (Fig. 2c,d). CRS was more frequent in responders. CRS occurred in 89% of patients with PR, 47% with SD and 43% with progressive disease (PD).

Objective responses were not observed in the two patients with SS who received a second infusion of afami-cel (Fig. 2a).

In the 16 heavily pre-treated metastatic SS patients, ORR was 44% (95% CI: 19.8, 70.1) (Fig. 2a, inset, and Extended Data Fig. 3b), and DCR was 94% (seven PR and eight SD). The change in SLD of the target lesions over time for patients with SS is shown in Fig. 2b (inset). Median TTR was 6.4 weeks (95% CI: 6.1, 18.1), and median DoR was 28.1 weeks (95% CI: 12.3, not reached). All seven responding patients had high tumor MAGE-A4 H-scores >214 and were treated with afami-cel doses $>9.5 \times 10^9$, except one patient receiving 4.5×10^9 cells. Median PFS was 20.4 weeks (95% CI: 10.0, 52.1) (Fig. 2c, inset), and median OS was 58.1 weeks (95% CI: 36.3, not reached) (Fig. 2d, inset), with 81%, 44% and 13% alive at 6 months, 12 months and 18 months, respectively. Three patients were progression free for >12 months.

Because disease-specific mortality in SS is mediated by progression of pulmonary and pleural metastases, radiologically confirmed durable regression of intrathoracic lesions after afami-cel could suggest clinical benefit. For example, pre-infusion and post-infusion cross-sectional thoracic contrast computed tomography scans in two patients with SS (each with MAGE-A4 H-scores >200 , large baseline tumor burdens and treated with high afami-cel doses) confirmed the

in vivo potency and anti-tumor activity of afami-cel (Patients A and B; Extended Data Fig. 4 and Supplementary Table 5). Both patients had PRs with TTR at week 6 and SLD reductions of ~45% (at 12 weeks) and ~81% (at 6 weeks), respectively, principally in pleural metastasis target lesions (Extended Data Fig. 4 and Supplementary Table 5). In Patient A, afami-cel was associated with reductions in metastatic disease in hemithorax, including regression of a large left lung pleural metastasis that crossed the midline at baseline and re-expansion of the right lung, as shown on a computed tomography scan at week 12 after afami-cel (Extended Data Fig. 4), associated with patient-reported improvement in exertional dyspnea. In Patient B, afami-cel was associated with overall reduction in left lung pleural metastases, including complete resolution of one pleural metastasis (Extended Data Fig. 4).

Patients A and B were administered a second T cell infusion (manufactured from surplus cell material collected at the initial leukapheresis) after disease progression from their first afami-cel infusions. Neither of the second infusions led to a response. Baseline tumor biopsy before the second infusion in Patient A showed markedly lower MAGE-A4 expression compared with a tumor biopsy before the first infusion (H-score, 37 versus 214, respectively). For Patient B, MAGE-A4 expression was high in biopsies taken before the first and second infusions (Supplementary Table 5).

Translational analyses

Exploratory analyses aimed to evaluate peripheral and tumor profiles relating afami-cel, including its circulating persistence and pharmacodynamic immune markers, and the tumor microenvironment before infusion and after infusion. This included immunophenotyping and cytotoxicity of afami-cel manufactured product (MP), serum cytokine profiling and spatial protein and gene expression profiling of the tumor microenvironment.

Exploratory peripheral analyses. Afami-cel MP showed in vitro cytotoxic activity in all batches before dosing. In vitro killing of MAGE-A4⁺ tumor cells by CD8⁺ afami-cel was significantly greater compared with CD4⁺ afami-cel (at 72 hours: median, 79.9% (range, 33.5–97.6%; $n = 37$) versus median, 6.6% (range, –8.7% to 52.9%; $n = 35$), respectively; $P = 5.8 \times 10^{-11}$ (paired Wilcoxon test)). The immunophenotype profile, examined for 33 patient MP samples showed transduced CD4⁺ to CD8⁺ cell ratios between 16.16 (CD4-biased) and 0.03 (CD8-biased) (median, 1.81), with no significant association with clinical response (Extended Data Fig. 5a). Infused MPs had CD4⁺ and CD8⁺ afami-cel predominantly resembling effector memory cells (T_{EM} ; CCR7[−]CD45RA[−]) (median, 69.5% and 56.5%, respectively) and terminally differentiated effector memory cells (T_{EMRA} ; CCR7[−]CD45RA⁺) (median, 23.3% and 36%, respectively). Stem cell memory (T_{SCM} ; CD45RA⁺CCR7[−]) and central memory (T_{CM} ; CD45RA⁺CCR7⁺) subsets were less frequent in the infused MPs (generally <10% and <15%, respectively). No association was observed between prevalence of these subsets and clinical response (Extended Data Fig. 5b).

Persistence of afami-cel was detected in all post-infusion blood samples up to 18 months after treatment. Peak afami-cel persistence was reached in most patients within the first 7 days after infusion.

Integration site analysis evaluated clonality status. In five patients with persistence >1% of peripheral blood mononuclear cells (PBMCs) 1 year after infusion, afami-cel showed a high level of polyclonality and absence of clonal dominance (Supplementary Table 7).

To assess whether long-term persisting afami-cel retains its functional cytolytic capacity, a sample was taken ~9 months after afami-cel infusion from a patient with SS with durable PR for 28 weeks who eventually progressed. CD8⁺ afami-cel retained its functional capacity for HLA-directed tumor cell lysis in vitro (75% of targets killed in 72 hours, 93% killed in 125 hours), suggesting that loss of response in this patient was not associated with loss of CD8⁺ T cell function.

Longitudinal changes in memory subset populations in the transduced CD4⁺ and CD8⁺ afami-cel pool were profiled in post-infusion PBMC samples. A gradual increase in the proportion of circulating cells with a T_{SCM} phenotype and sustained presence of T_{EMRA} cell types was observed (Extended Data Fig. 6).

A panel of 22 serum cytokines was simultaneously assessed in mITT patient samples collected before infusion and after infusion to understand potential mechanisms of toxicity and efficacy. A transient post-infusion increase was evident for most serum cytokines across all patients, with the largest increases in interferon γ (IFN γ) levels. Serum IFN γ (Fig. 3a), interleukin 6 (IL-6) (Extended Data Fig. 7a) and granulocyte–macrophage colony-stimulating factor (GM-CSF) (Extended Data Fig. 7b) levels were relatively greater in patients with Grade ≥ 3 CRS versus Grade ≤ 2 CRS and without CRS (Supplementary Table 8).

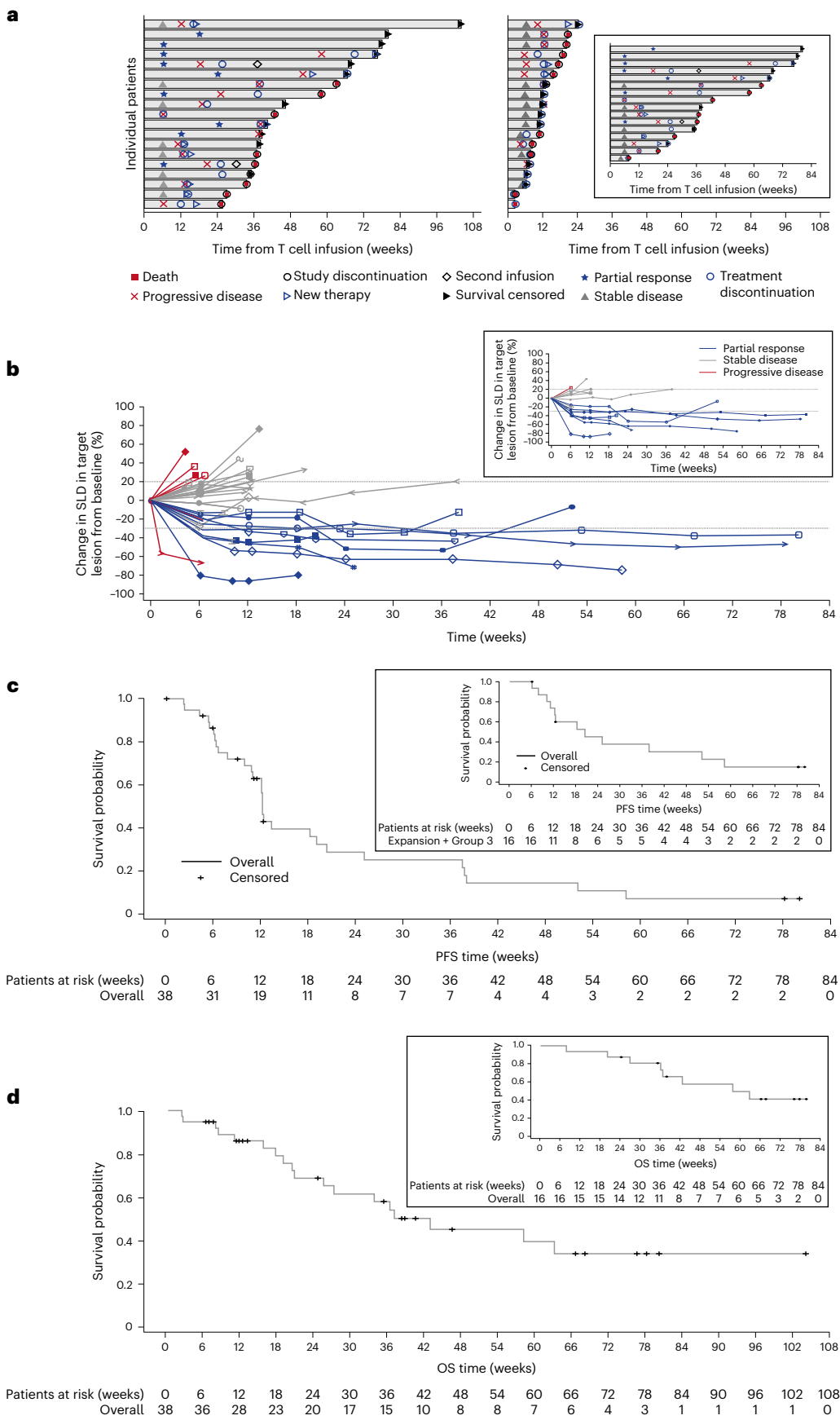
Analyses of serum cytokine relationships with clinical response showed a significant correlation between peak serum IFN γ levels and tumor reduction (Fig. 3b). Peak serum IFN γ levels were significantly greater in responders than non-responders (Fig. 3c). No significant difference was noted among PD, SD and not evaluable (NE) patient subsets. As anticipated for the mechanism of action for LD chemotherapy¹⁰, serum IL-15 concentrations increased in post-LD versus pre-LD samples, but there was no difference in serum IL-15 concentrations between the two LD chemotherapy regimens. The median post-LD versus pre-LD ratio of IL-15 was 18.25 for the high LD group and 12.87 for the low LD group ($P = 0.13$ (two-sided Wilcoxon test)) (Extended Data Figs. 8 and 9).

Further pharmacodynamic analyses of afami-cel were supported by the evaluation of 92 immuno-oncology-related serum proteins using Olink technology. Markers with the greatest afami-cel infusion-related changes included IFN γ and related markers. After afami-cel, fold increases in serum IFN γ levels relative to baseline were associated with anti-tumor response; this was more evident in SS than other tumors (Fig. 3d). Overall, peak levels of 14 serum markers after treatment correlated with tumor reduction, and serum IFN γ levels showed the largest positive correlation (Supplementary Table 9).

Exploratory tumor analyses. Infiltration of non-transduced T cells and afami-cel was evaluated in 24 post-infusion biopsies from 16 patients treated in the expansion phase (Extended Data Fig. 10a). CD3⁺ cells were detected in all samples (range, 4–1,891 CD3⁺ cells per mm² (median, 90)), with afami-cel evident in 67% of samples (16/24; range, 0–385 transduced T cells per mm² (median, 2.3)), including biopsies obtained at study completion and autopsy. Of biopsies without afami-cel

Fig. 2 | Response and prognostic characteristics of the mITT population and patients with SS. **a**, Swimmer's plot of patient response over time in the mITT population ($N = 38$). The inset is response over time in patients with SS ($n = 16$). **b**, DoR profiles show the change from baseline in target lesions using RECIST version 1.1 in the overall treatment group after first infusion for responders and non-responders. The inset shows the change from baseline in target lesions in patients with SS. The probability of DoR was 100% (95% CI: 100, 100) at ≥ 12 weeks and 60% (95% CI: 20.4, 80.5) at ≥ 24 weeks. Duration of stable disease probability at ≥ 24 weeks for patients with SS was 50% (95% CI: 22.5%, 75.0%). **c**, Kaplan–Meier curves show PFS in the mITT population. The inset shows the PFS curve for the patients with SS. The median PFS for the mITT population was 12.3 weeks (95% CI:

10.9, 19.1) and 20.4 weeks (95% CI: 10.0, 52.1) for the patients with SS. PFS events in the mITT population included 25 events (65.8%) of PD and four events (10.5%) of death. PFS probability was 60% (95% CI: 44.8, 76.6) at 12 weeks and 30% (95% CI: 14.1, 45.2) at 24 weeks. PFS probability in the patients with SS was 70% (95% CI: 0.44, 0.89) at 12 weeks and 50% (95% CI: 0.19, 0.68) at 24 weeks. **d**, Kaplan–Meier curves show OS in the mITT population. The inset shows the OS for patients with SS. The median OS for the mITT population was 42.9 weeks (95% CI: 20.7, not reached) and 58.1 weeks (95% CI: 36.3, not reached) for patients with SS. OS probability was 90% (95% CI: 69.8, 94.0) at 12 weeks and 70% (95% CI: 49.6, 82.1) at 24 weeks. OS probability in patients with SS was 90% (95% CI: 0.63, 0.99) at 12 weeks and remained 90% (95% CI: 0.59, 0.97) at 24 weeks.



detection, seven of eight were taken at study completion. Biopsies were taken from 6 weeks to 93 weeks (median, 67) after infusion and compared with the earlier biopsies taken from 6 weeks to 67 weeks (median, 12) from samples with afami-cel detected; MAGE-A4 expression was similar in both.

To examine the tumor microenvironment for patients with a differential response to afami-cel after receiving similar (high) cell doses ($9.0-10 \times 10^9$ transduced T cells), a sample set including on-study and at-completion biopsies from four patients across two tumor types (Patients 1, 2 and 3 had SS and Patient 4 had ovarian cancer; Extended Data Fig. 10a) was prioritized for multiplex immunofluorescence analyses. Compared with baseline, relatively greater intra-tumoral detection of proliferating (Ki67⁺) and/or activated (granzyme B⁺ and PD-L1⁺) T cells (CD4, CD8 and 'regulatory') was evident after afami-cel in on-study (Patient 1) and at-completion/withdrawal (Patient 2) biopsies, in line with afami-cel detection. For Patient 3, a relatively lower intra-tumoral detection of proliferating and/or activated T cells was observed at completion compared with the on-study biopsy, consistent with low/negligible afami-cel detection (Fig. 4a). At baseline, an ovarian tumor biopsy (Patient 4) had a relatively higher presence of T cell phenotypes compared with SS tumor biopsies (Patients 1 and 2). Post-infusion ovarian tumor biopsy (Patient 4) also showed a high level of afami-cel infiltrates (Fig. 4b, panel B) in areas that corresponded spatially with those showing the presence of cytotoxic and regulatory T cells near malignant cells (Fig. 4b, panels A and C).

The absence of a clinical response in Patient 4, despite high-dose afami-cel (9.4×10^9 transduced cells) and evidence of high levels of intra-tumoral immune cell infiltration (including afami-cel), could possibly be explained by the presence of immunosuppressive markers.

NanoString nCounter analyses showed that intra-tumoral gene expression levels encoding T cell exhaustion markers (that is, LAG-3, TIGIT, CTLA-4 and PD-1) and immunosuppressive markers, including arginase (for which serum levels were negatively correlated with clinical response), were relatively higher in biopsy from Patient 4 (on-treatment greater than baseline) compared with SS samples (Fig. 4c). Furthermore, a gene set variation analysis comparing scores for PanCancer Immune Profiling Panel categories also indicated differences between Patient 4 (ovarian cancer) and patients with SS. The former showed negative enrichment for natural killer cells and central and effector memory T cells and positive enrichment for cytotoxic cells and type 17 helper T cells, contrasting with SS samples (Extended Data Fig. 10b).

Discussion

In this phase 1 trial, we evaluated the safety, clinical activity and translational effects of afami-cel in HLA-A*02⁺ patients with MAGE-A4-expressing solid tumors. Prolonged cytopenia, CRS and neurotoxicity were three TEAEs of special interest. The prolonged cytopenia-related fatality in a patient with SS caused by aplastic anemia might have been caused by the higher LD dose of $3,600 \text{ mg/m}^2$ of cyclophosphamide. Because this patient also had two sequential high-grade CRS events, it cannot be excluded that there was a contributory systemic

inflammatory component to this Grade 5 event. Reassuringly, there was no evidence of an off-tumor, on-target effect observed in the bone marrow because MAGE-A4 expression was absent. However, although 45% of patients had at least one prolonged Grade ≥ 3 cytopenia, the incidence of clinical sequelae, including systemic infections, was low. Overall, the lower-dose cyclophosphamide LD regimen was associated with a favorable hematological toxicity profile and a similar serum IL-15 profile compared to patients treated with the higher-dose cyclophosphamide LD regimen. Given the overall favorable hematological safety profile of fludarabine $30 \text{ mg/m}^2 \times 4$ days and cyclophosphamide $600 \text{ mg/m}^2 \times 3$ days LD chemotherapy and its ability to support afami-cel anti-tumor activity across different indications, with no discernable difference in serum IL-15 levels compared to the higher cyclophosphamide dose schedule, the lower LD chemotherapy regimen was selected for the registration-directed phase 2 SPEARHEAD-1 trial (NCT04044768).

Afami-cel-related CRS occurred in 55% of all patients and was typically low-grade, early-onset, post-infusion and reversible in all cases with the administration of anti-IL-6(R) monoclonal antibody treatment when indicated. Consistent with the known monocyte-macrophage-centric pathophysiology of CRS, elevations in serum cytokines (including IFN γ , IL-6 and GM-CSF) were associated with increasing CRS grades. The overall incidence and severity of ICANS/encephalopathy was low, with no reported cases in patients with SS. Although additional neurological AEs were reported across tumor types, there was no consistent pattern to suggest a definite causal relationship with afami-cel. The safety findings reported here are consistent with those observed in patients with cancer undergoing LD chemotherapy and cellular therapy, including treatment with chimeric antigen receptor T cells or NY-ESO-1 T cells¹¹⁻¹³.

Patients treated in the trial had nine different cancers with heterogeneous MAGE-A4 expression, and most patients with therapeutic responses had high H-scores. The ORR of 24% in the overall population was primarily due to clinical activity observed in SS. Responses were limited in non-sarcoma cancers, perhaps due to small numbers of patients with specific cancer types or lower MAGE-A4 expression relative to SS. Although the number of patients with SS was small, the emergent ORR of 44%, median PFS of 20.4 weeks and median OS of 58.1 weeks are better than the historical low ORRs reported for current standard-of-care therapies, including pazopanib and trabectedin, used in the post-first-line metastatic setting^{14,15}. SS is sensitive to alkylators, and the use of cyclophosphamide in the LD regimen is a confounder in the interpretation of the response rate in SS.

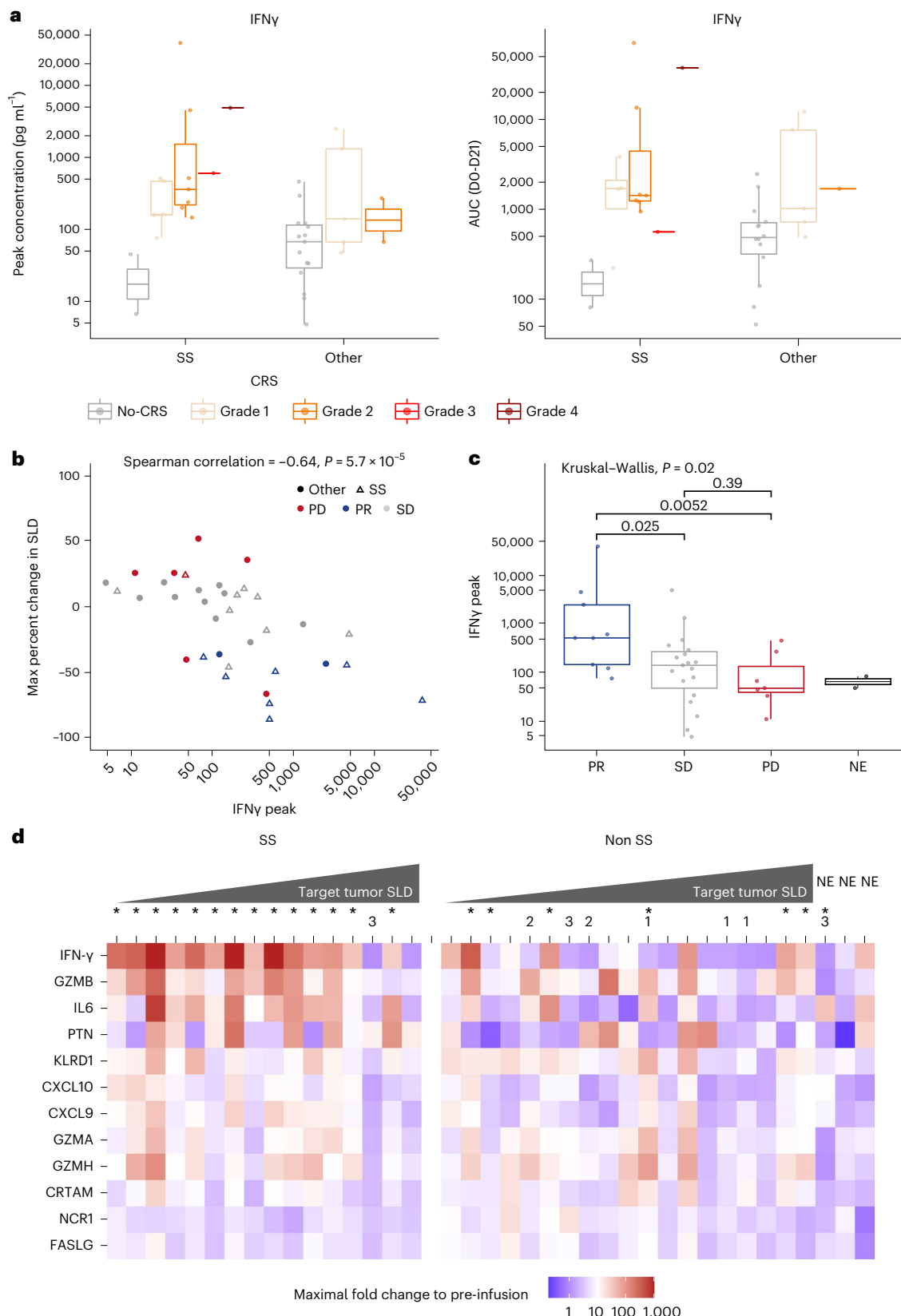
Preliminary evaluation of pharmacokinetic and pharmacodynamic relationships associated with afami-cel dose escalation used peak cell persistence and peak serum IFN γ levels as prototypical pharmacokinetic and pharmacodynamic markers, respectively. When considering the subset of patients with ovarian cancer across all dosing groups, increases in afami-cel doses were associated with progressively increasing peak cell persistence and peak IFN γ levels (Supplementary Table 10). Although cyclophosphamide-containing LD chemotherapy, or persisting therapeutic effects of bridging therapy, may have

Fig. 3 | Serum IFN γ patient profiles and associations between peak and AUC concentrations of IFN γ levels and anti-tumor response. **a**, Comparison of serum levels in patients with SS (no CRS $n = 2$, Grade 1 $n = 5$, Grade 2 $n = 7$, Grade 3 $n = 1$, Grade 4 $n = 1$) and those with other indications (no CRS $n = 15$, Grade 1 $n = 5$, Grade 2 $n = 2$) across CRS groups. Peak IFN γ levels (pg ml^{-1}) were significantly greater in patients with CRS (all grades, $n = 21$) compared with non-CRS ($n = 17$) (median, 270.8 pg ml^{-1} and 47.7 pg ml^{-1} , respectively; $P = 0.00012$). Calculated IFN γ AUC from days 0 to 21 was significantly greater in patients with CRS compared with non-CRS (median, $1,455.0 \text{ pg ml}^{-1}$ and 467.0 pg ml^{-1} , respectively; $P = 0.00061$) (Wilcoxon rank-sum test, two-sided). **b**, Serum IFN γ concentration (pg ml^{-1}) measured across sample sets collected on days 0–21 after infusion. Magnitude of maximum percent change in SLD was positively correlated with reduction in target tumor lesion (Spearman's $r = -0.64$; $P = 0.000057$).

c, Peak serum IFN γ levels were significantly greater in patients with best overall responses of PR ($n = 9$) compared with PD ($n = 7$; $P = 0.0052$) and SD ($n = 19$; $P = 0.025$) (Kruskal–Wallis test, two-sided). **d**, Patients ranked by best percent change in SLD. Non-SS subset included three NE patients. The asterisk in superscript (*) indicates CRS; number indicates dose-escalation cohort. AUC, area under the curve; CRTAM, class I-restricted T cell-associated molecule; CXCL, chemokine (C-X-C motif) ligand; FASLG, FAS ligand; IQR, interquartile range; KLRD1, killer cell lectin like receptor D1; NC1, natural cytotoxicity triggering receptor 1; PTN, pleiotrophin. Box plots depict median as horizontal lines within boxes, with box bounds as the first and third quartiles. Dots represent individual data points. Lower whiskers are minimum values within 1.5 times the IQR below the 25th percentile. Upper whiskers are maximum values within 1.5 times the IQR above the 75th percentile.

contributed to disease control in ovarian cancer and SS, the independent therapeutic activity of afami-cel in responding patients is corroborated by cell pharmacokinetic and serum pharmacodynamic findings. The durable reduction in SLD for several months in some patients with SS after one afami-cel infusion suggests that the anti-tumor effect

of afami-cel lasts longer than would be expected after one cycle of alkylating-agent-containing LD chemotherapy. Although some patients with PD had rapidly decreasing levels of afami-cel persistence, some maintained high levels of persistence, suggesting that tumor-intrinsic factors, possibly immuno-editing mechanisms (for example, loss of



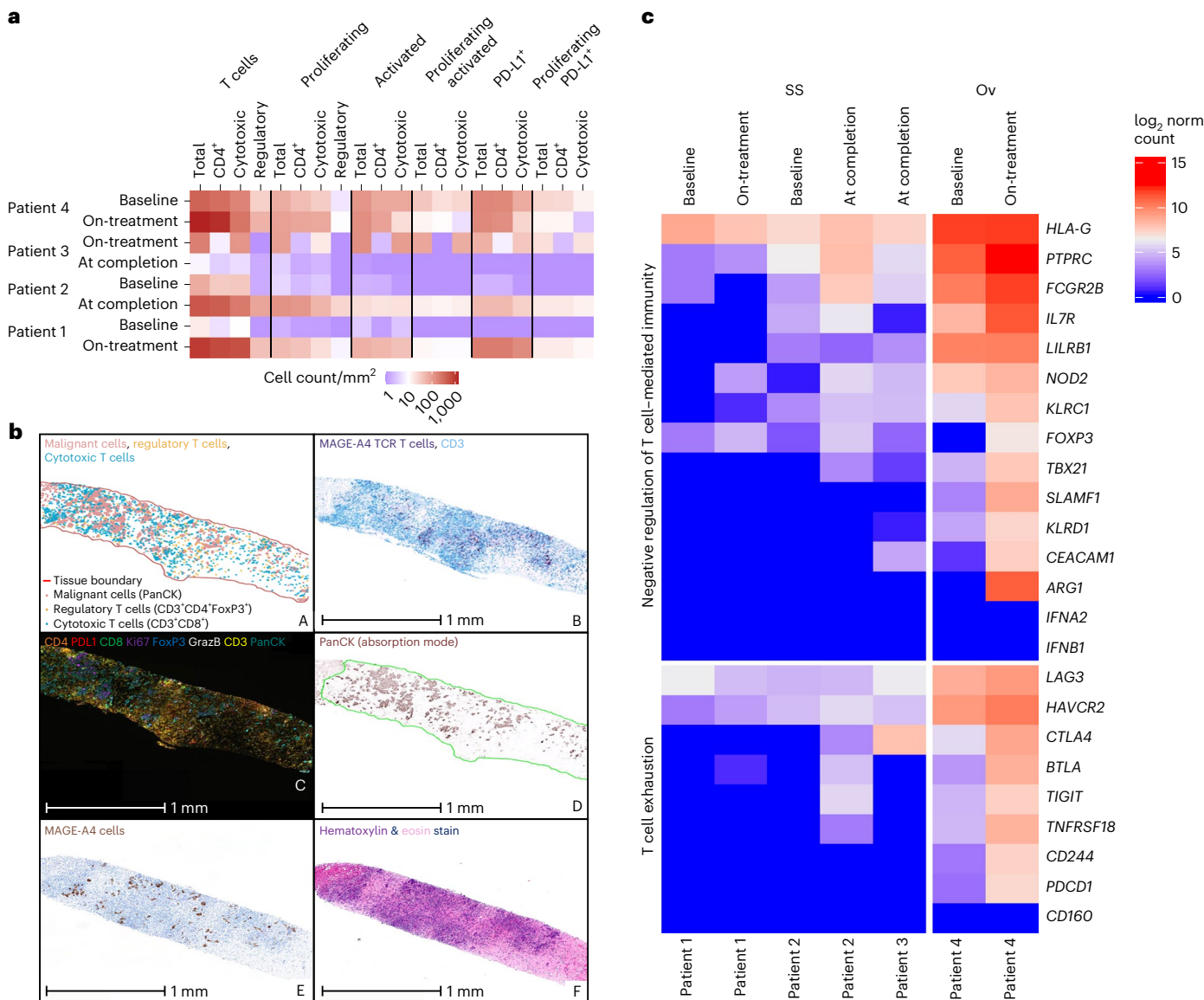


Fig. 4 | Detection of afami-cel and T cell phenotypes in patient tumor biopsies. **a**, Digital image quantification of T cell markers (total CD3⁺), CD4 (CD3⁺CD4⁺), cytotoxic (CD3⁺CD8⁺), regulatory (CD3⁺CD4⁺FoxP3⁺) and co-staining for phenotypes (proliferating, Ki67⁺; activated, GrazB⁺; PD-L1⁺) and combination of these phenotypes for the four patients referenced in Extended Data Fig. 10a. Baseline biopsies were taken 2–5 weeks before afami-cel infusion. **b**, A multiparametric analysis of T cell infiltration in tumor biopsies using IHC, MAGE-A4 SPEAR RNAscope (Advanced Cell Diagnostics) and multiplex immunofluorescence. Images of post-infusion biopsy (liver) from Patient 4: A, spatial plot generated using spatial analysis module in HALO (Indica Labs) showing malignant cells (PanCK⁺ (red)), regulatory (CD3⁺CD4⁺FoxP3⁺) T cells (yellow) and cytotoxic (CD3⁺CD8⁺) T cells (blue/cyan)). Scale bar is not applicable as this is not a raw image; B, CD3 IHC/SPEAR T cell RNAscope duplex

(CD3 IHC staining (blue); MAGE-A4 SPEAR T cell staining (purple)); C, Ultivue 8-plex multiplex dataset showing CD4 (orange), PD-L1 (red), CD8 (green), Ki67 (purple), FoxP3 (blue), GrazB (white), CD3 (yellow) and PanCK (teal); D, PanCK immunofluorescence staining from Ultivue 8-plex panel (displayed in absorption mode in HALO for clarity); E, MAGE-A4 IHC stain (DAB (brown)); and F, hematoxylin (purple) and eosin (pink) stain. **c**, Heat map of log₂-transformed normalized counts of genes associated with 'T cell exhaustion' and 'Negative regulation of T cell-mediated immunity' in baseline and post-infusion biopsies from Patients 1–4. Patients 1–3 were patients with SS; Patient 4 was a patient with ovarian cancer. DAB, 3,3'-diaminobenzidine; FoxP3, forkhead box protein 3; GrazB, granzyme B; Ov, ovarian; PanCK, pancytokeratin; PD-L1, programmed death ligand 1.

MAGE-A4 or HLA expression), or potential immunosuppressive factors (such as arginase-1), might contribute to the development of afami-cel resistance even if afami-cel cytolytic activity can be maintained *in vivo*.

The serum cytokine response profile indicated an IFN γ -driven mechanism of action as well as emerging biomarkers of anti-tumor response. Tumor analyses supported the co-localization of afami-cel with cancer cells and resident immune cells in tumors, with evidence of activated and proliferative intra-tumoral T cell states and adaptive immune responses. Because the ongoing phase 2 SPEARHEAD-1 trial

will have dosed ~100 patients with SS and MRCLS with afami-cel at completion, confirmation of these preliminary translational analyses may be possible in future pooled analyses. This will include a deeper evaluation of the potentially complex inter-relationship between immunological components of the tumor microenvironment and dynamic temporal changes in afami-cel phenotype and function after infusion.

In summary, our findings demonstrate that afami-cel was well tolerated and suggest that it could be a promising therapy for patients with metastatic SS who have received prior ifosfamide treatment.

Limitations to the interpretation of the response rate in SS include the small sample size and confounding effect of LD. Nevertheless, the encouraging results warrant further study, and additional data in metastatic SS will be evaluated in the phase 2 SPEARHEAD-1 trial¹⁶. Investigation into next-generation T cell therapies with enhanced cytolytic and immunological properties for a range of MAGE-A4⁺ epithelial solid tumors has commenced (NCT04044859 and NCT04752358).

Online content

Any methods, additional references, Nature Portfolio reporting summaries, source data, extended data, supplementary information, acknowledgements, peer review information; details of author contributions and competing interests; and statements of data and code availability are available at <https://doi.org/10.1038/s41591-022-02128-z>.

References

1. Caballero, O. L. & Chen, Y. T. Cancer/testis (CT) antigens: potential targets for immunotherapy. *Cancer Sci.* **100**, 2014–2021 (2009).
2. Daudi, S. et al. Expression and immune responses to MAGE antigens predict survival in epithelial ovarian cancer. *PLoS ONE* **9**, e104099 (2014).
3. Sharma, P. et al. Cancer-testis antigens: expression and correlation with survival in human urothelial carcinoma. *Clin. Cancer Res.* **12**, 5442–5447 (2006).
4. Ishihara, M. et al. MAGE-A4, NY-ESO-1 and SAGE mRNA expression rates and co-expression relationships in solid tumours. *BMC Cancer* **20**, 606 (2020).
5. Iura, K. et al. Cancer-testis antigen expression in synovial sarcoma: NY-ESO-1, PRAME, MAGEA4, and MAGEA1. *Hum. Pathol.* **61**, 130–139 (2017).
6. Tawbi, H. A. et al. Pembrolizumab in advanced soft-tissue sarcoma and bone sarcoma (SARC028): a multicentre, two-cohort, single-arm, open-label, phase 2 trial. *Lancet Oncol.* **18**, 1493–1501 (2017).
7. Italiano, A., Bellera, C. & D'Angelo, S. PD1/PD-L1 targeting in advanced soft-tissue sarcomas: a pooled analysis of phase II trials. *J. Hematol. Oncol.* **13**, 55 (2020).
8. Sanderson, J. P. et al. Preclinical evaluation of an affinity-enhanced MAGE-A4-specific T-cell receptor for adoptive T-cell therapy. *Oncoimmunology* **9**, 1682381 (2020).
9. Ramachandran, I. et al. Systemic and local immunity following adoptive transfer of NY-ESO-1 SPEAR T cells in synovial sarcoma. *J. Immunother. Cancer* **7**, 276 (2019).
10. Anthony, S. M. et al. Inflammatory signals regulate IL-15 in response to lymphodepletion. *J. Immunol.* **196**, 4544–4552 (2016).
11. D'Angelo, S. P. et al. Antitumor activity associated with prolonged persistence of adoptively transferred NY-ESO-1 c259T cells in synovial sarcoma. *Cancer Discov.* **8**, 944–957 (2018).
12. Neelapu, S. S. et al. Axicabtagene ciloleucel CAR T-cell therapy in refractory large B-cell lymphoma. *N. Engl. J. Med.* **377**, 2531–2544 (2017).
13. Maude, S. L. et al. Tisagenlecleucel in children and young adults with B-cell lymphoblastic leukemia. *N. Engl. J. Med.* **378**, 439–448 (2018).
14. Desar, I. M. E., Fleuren, E. D. G. & van der Graaf, W. T. A. Systemic treatment for adults with synovial sarcoma. *Curr. Treat. Options Oncol.* **19**, 13 (2018).
15. Carroll, C. et al. Meta-analysis of pazopanib and trabectedin in 2L+ metastatic synovial sarcoma (2L+ mSS). *Cancer Res.* **81**, 2630 (2021).
16. D'Angelo, S. P. et al. SPEARHEAD-1: a phase 2 trial of afamitresgene autoleucel (formerly ADP-A2M4) in patients with advanced synovial sarcoma or myxoid/round cell liposarcoma. *J. Clin. Oncol.* **39**, 11504 (2021).

Publisher's note Springer Nature remains neutral with regard to jurisdictional claims in published maps and institutional affiliations.

Open Access This article is licensed under a Creative Commons Attribution 4.0 International License, which permits use, sharing, adaptation, distribution and reproduction in any medium or format, as long as you give appropriate credit to the original author(s) and the source, provide a link to the Creative Commons license, and indicate if changes were made. The images or other third party material in this article are included in the article's Creative Commons license, unless indicated otherwise in a credit line to the material. If material is not included in the article's Creative Commons license and your intended use is not permitted by statutory regulation or exceeds the permitted use, you will need to obtain permission directly from the copyright holder. To view a copy of this license, visit <http://creativecommons.org/licenses/by/4.0/>.

© The Author(s) 2023

David S. Hong  ^{1,17}, Brian A. Van Tine  ^{2,17}, Swethajit Biswas³, Cheryl McAlpine³, Melissa L. Johnson⁴, Anthony J. Olszanski  ⁵, Jeffrey M. Clarke⁶, Dejka Araujo⁷, George R. Blumenschein Jr⁸, Partow Kebriaei⁹, Quan Lin¹⁰, Alex J. Tipping³, Joseph P. Sanderson  ³, Ruoxi Wang³, Trupti Trivedi¹⁰, Thejo Annareddy¹⁰, Jane Bai¹⁰, Stavros Rafail¹⁰, Amy Sun¹⁰, Lilliam Fernandes³, Jean-Marc Navenot¹⁰, Frederic D. Bushman  ¹¹, John K. Everett¹¹, Derin Karadeniz¹¹, Robyn Broad³, Martin Isabelle³, Revashnee Naidoo³, Natalie Bath³, Gareth Betts³, Zohar Wolchinsky³, Dzmitry G. Batrakou³, Erin Van Winkle¹⁰, Erica Elefant¹⁰, Armin Ghobadi², Amanda Cashen², Anne Grand'Maison¹², Philip McCarthy¹², Paula M. Fracasso  ¹⁰, Elliot Norry¹⁰, Dennis Williams¹⁰, Mihaela Druta¹³, David A. Liebner¹⁴, Kunle Odunsi  ¹⁵ & Marcus O. Butler  ¹⁶

¹Department of Investigational Cancer Therapeutics, Division of Cancer Medicine, The University of Texas MD Anderson Cancer Center, Houston, TX, USA. ²Section of Medical Oncology, Division of Oncology, Siteman Cancer Center, Washington University School of Medicine, St. Louis, MO, USA.

³Adaptimmune, Abingdon, Oxfordshire, UK. ⁴Sarah Cannon Cancer Institute, Tennessee Oncology/One Oncology, Nashville, TN, USA. ⁵Department of Hematology/Oncology, Fox Chase Cancer Center, Philadelphia, PA, USA. ⁶Duke Cancer Institute, Duke University, Durham, NC, USA. ⁷Department of Sarcoma Medical Oncology, Division of Cancer Medicine, The University of Texas MD Anderson Cancer Center, Houston, TX, USA. ⁸Department of Thoracic-Head and Neck Medical Oncology, Division of Cancer Medicine, The University of Texas MD Anderson Cancer Center, Houston, TX, USA.

⁹Department of Stem Cell Transplantation and Cellular Therapy, Division of Cancer Medicine, The University of Texas MD Anderson Cancer Center, Houston, TX, USA. ¹⁰Adaptimmune, Philadelphia, PA, USA. ¹¹Department of Microbiology, University of Pennsylvania, Philadelphia, PA, USA. ¹²Department of Medicine, Roswell Park Comprehensive Cancer Center, Buffalo, NY, USA. ¹³Sarcoma Medical Oncology, Moffitt Cancer Center, Tampa, FL, USA.

¹⁴Department of Internal Medicine, Division of Medical Oncology, and Department of Biomedical Informatics, Division of Computational Biology and Bioinformatics, Ohio State University, Columbus, OH, USA. ¹⁵University of Chicago Medicine Comprehensive Cancer Center, Chicago, IL, USA.

¹⁶Department of Medical Oncology and Hematology, Princess Margaret Cancer Centre, University of Toronto, Toronto, Canada. ¹⁷These authors contributed equally: David S. Hong, Brian A. Van Tine. e-mail: dshong@mdanderson.org;

Methods

Study design and participants

This open-label, phase 1 trial was conducted at multiple centers in North America to evaluate the safety of afami-cel in HLA-A*02⁺ patients with MAGE-A4-expressing solid cancers.

All patients underwent two pre-screening evaluations using different screening protocols ([NCT02636855](#)): (1) HLA testing for at least one HLA-A2 inclusion allele (HLA-A*02:01, HLA-A*02:02, HLA-A*02:03, HLA-A*02:06 or HLA-A*02:09) and absence of the exclusion allele HLA-A*02:05; and (2) MAGE-A4 tumor biopsy testing using an anti-MAGE-A4 immunohistochemistry (IHC) assay (Supplementary Table 1). Only patients with an appropriate HLA-A2 genotype and whose tumor expressed the MAGE-A4 antigen above the specified cutoff level were eligible to undergo screening for this study.

Inclusion criteria

Patients must have voluntarily agreed to participate by giving written informed consent in accordance with International Council on Harmonization (ICH) Good Clinical Practice (GCP) guidelines and applicable local regulations. Patients must have agreed to abide by all protocol-required procedures, including study-related assessments and management by the treating institution for the duration of the study and LTFU phase. Patients were ≥ 18 years to ≤ 75 years of age at the time of signing the study informed consent.

Patients must have had histologically confirmed diagnosis of any one of the following cancers: (1) urothelial cancer (transitional cell cancer of the bladder, ureter, urethra or renal pelvis); (2) melanoma; (3) squamous cell carcinoma of the head and neck; (4) ovarian cancer; (5) NSCLC (squamous, adenosquamous, adenocarcinoma or large cell); (6) esophageal cancer (squamous and adenocarcinoma); (7) gastric cancer; (8) SS; or (9) MRCLS. Patients must have had measurable disease according to RECIST version 1.1 criteria before LD. Measurable disease was not required before leukapheresis. Patients must have had the following disease-specific requirements for their tumor type (note: there was no limit to the number of therapies before study entry). (1) Inoperable or metastatic (advanced) urothelial cancer: patients must have received at least one prior systemic therapy in the adjuvant or metastatic setting; may have received treatment with a programmed cell death protein 1 (PD-1) or programmed death-ligand 1 (PD-L1) inhibitor. (2) Inoperable or metastatic (advanced) melanoma: patients must have received, were intolerant to or refused a cytotoxic T lymphocyte-associated protein 4 inhibitor (ipilimumab) or a PD-1 inhibitor (nivolumab or pembrolizumab) as monotherapy or a combination of ipilimumab and nivolumab. Patients must have received or were intolerant to a B-Raf proto-oncogene (BRAF) inhibitor or the combination of BRAF and mitogen-activated protein kinase inhibitors for BRAF(V600) mutant melanoma. (3) Inoperable or metastatic (advanced) squamous cell head and neck cancer: patients must have received a platinum-containing chemotherapy for treatment of primary tumor in adjuvant, locally advanced or metastatic settings, were intolerant to or refused such treatment. They may have received prior immunotherapy. (4) Inoperable or metastatic (advanced) ovarian, primary peritoneal or fallopian tube carcinoma: patients must have received platinum-containing chemotherapy and had platinum-refractory or platinum-resistant disease. If platinum-sensitive disease, patients should have received at least two lines of chemotherapy. Patients may have received poly(adenosine diphosphate-ribose) polymerase inhibitors, bevacizumab or immunotherapy. (5) Histologically or cytologically confirmed diagnosis of advanced NSCLC (Stage IIIB or Stage IV) or recurrent disease (squamous, adenosquamous, adenocarcinoma or large cell carcinoma): patients whose tumors were known to have epidermal growth factor receptor (EGFR) mutations or anaplastic lymphoma kinase (ALK) gene rearrangements must have failed (PD or unacceptable toxicity) prior EGFR inhibitor or ALK tyrosine kinase inhibitor, respectively. Patients with ROS-1⁺ tumors must have failed an

ALK inhibitor (crizotinib). Patients had received or are receiving at least one line of prior therapy. Patients may have received PD-1 inhibitors. There was no limit on lines of prior anti-cancer therapies. (6) Inoperable or metastatic (advanced) squamous or adenocarcinoma of the esophagus, gastroesophageal junction or gastric cancer: patients must have received, were intolerant to or refused at least one fluorouracil (5-FU) and/or platinum-containing regimen. Patients whose tumors were known to have HER2/neu amplification must have failed (PD or unacceptable toxicity) or refused trastuzumab. Patients may have received ramucirumab. (7) Advanced (metastatic or inoperable) SS or high-grade MRCLS confirmed by histology or cytogenetics: patients with SS must have previously received an anthracycline-containing regimen. Patients who were intolerant to anthracycline may have received ifosfamide alone. Patients with MRCLS must have previously received or be intolerant to an anthracycline-containing regimen.

Patients were HLA-A*02⁺ (this determination was made under screening protocol ADP-0000-001). The sponsor reviewed the results of HLA typing for inclusion and exclusion alleles and adjudicated patient eligibility based on HLA results. Patients' tumors (either an archival specimen or a fresh biopsy) showed expression of the MAGE-A4 RNA or protein. All samples must have been reviewed by an Adaptimmune-designated central laboratory confirming expression. Patients had anticipated life expectancy of >6 months before leukapheresis and >3 months before LD. Patients had an Eastern Cooperative Oncology Group (ECOG) performance status of 0–1. Patients had a left ventricular ejection fraction $\geq 50\%$. Patients were fit for leukapheresis and had adequate venous access for the cell collection. Female patients of childbearing potential (FCBPs) must have had a negative urine or serum pregnancy test (note: FCBP was defined as pre-menopausal and not surgically sterilized). FCBPs must have agreed to use maximally effective birth control or to abstain from heterosexual activity throughout the study, starting at the first dose of chemotherapy, for 12 months after receiving the investigational product or 4 months after there was no evidence of persistence/gene-modified cells in the patient's blood, whichever was longer. Male patients must have been surgically sterile or agreed to use a double-barrier contraception method or abstain from heterosexual activity with an FCBP starting at the first dose of chemotherapy and for 4 months thereafter. Patients must have had adequate organ function as indicated by laboratory values (Supplementary Table 11).

Exclusion criteria

Patients who were HLA-A*02:05⁺ in either allele, those with HLA-A*02:07 as the sole HLA-A*02 allele and those with any A*02 null allele (designated with an 'N'; for example, A*02:32N) as the sole HLA-A*02 allele were excluded from participating in the study. Patients must not have received or planned to receive excluded therapy/treatment before leukapheresis or LD chemotherapy (Supplementary Table 12). Patients with toxicity from previous anti-cancer therapy must have recovered to Grade ≤ 1 before enrollment (except for non-clinically significant toxicities—for example, alopecia and vitiligo). Patients with Grade 2 toxicities that were deemed stable or irreversible (for example, peripheral neuropathy) could have been enrolled.

Patients must not have had a history of allergic reactions attributed to compounds of similar chemical or biologic composition to fludarabine, cyclophosphamide or other agents used in the study. Patients must not have had a history of chronic or recurrent (within the last year before screening) severe autoimmune or immune-mediated disease requiring steroids or other immunosuppressive treatments, including anti-tumor necrosis factor (TNF) agents. Patients must not have had major surgery within 4 weeks before LD; patients should have been fully recovered from any surgical-related toxicities.

Patients with a prior history of symptomatic central nervous system (CNS) metastases must have received treatment (that is, stereotactic radiosurgery (SRS), whole-brain radiation therapy (WBRT)

or surgery) and been neurologically stable for ≥ 1 month, not requiring anti-seizure medications and off steroids for ≥ 14 days before leukapheresis and LD. Patients with asymptomatic CNS metastatic disease without associated edema, shift, requirement for steroids or anti-seizure medications were eligible. If such a patient received SRS or WBRT, a minimum period of 2 weeks would be needed to lapse between the therapy and LD. Patients with leptomeningeal disease or carcinomatous meningitis were not eligible. Patients must not have had any other active malignancy besides the tumor under study within 3 years before screening. Exceptions were adequately treated malignancies not likely to require therapy (for example, completely resected non-melanomatous skin carcinoma or successfully treated *in situ* carcinoma). Newly identified prostate cancers found during cytoprostatectomy were permitted. Patients must have been in complete remission from prior malignancy to be eligible to enter the study.

Patients must not have had an electrocardiogram (ECG) showing clinically significant abnormality at screening or showing an average corrected QT interval ≥ 450 ms in males and ≥ 470 ms in females (≥ 480 ms for patients with bundle branch block) over three consecutive ECGs. Either Fridericia's or Bazett's formula may have been used to correct the QT interval. Patients must not have had uncontrolled intercurrent illness, including, but not limited to, ongoing or active infection; clinically significant cardiac disease defined by New York Heart Association Class of Heart Failure >1 ; uncontrolled clinically significant arrhythmia in the last 6 months or acute coronary syndrome (angina or myocardial infarction) in the last 6 months; interstitial lung disease (pneumonitis); history of pneumectomy or chronic obstructive pulmonary disease with at least one exacerbation within 1 year before the screening visit that required treatment with systemic corticosteroids or resulted in hospitalization; pre-existing active skin disorders of Grade ≥ 2 severity; current uncontrolled hypertension despite optimal medical therapy; or a history of stroke or CNS bleeding, transient ischemic attack or reversible ischemic neurologic deficit within the last 6 months. Patients who, in the opinion of the investigator, were unlikely to fully comply with protocol requirements were ineligible. Patients must not have been pregnant or breastfeeding.

Patients must not have had active infection with human immunodeficiency virus (HIV), hepatitis B virus, hepatitis C virus (HCV) or human T-lymphotropic virus (HTLV). Patients with positive serology for HIV were excluded. Patients who were negative for hepatitis B surface antigen but positive for hepatitis B core antibody must have had undetectable hepatitis B DNA and received prophylaxis against viral reactivation. Prophylaxis should have been initiated before LD therapy and continued for 6 months. Patients who were positive for HCV antibody were screened for HCV RNA by any reverse transcription polymerase chain reaction (PCR) or branched DNA assay. If HCV antibody was positive, eligibility was determined based on a negative screening RNA value. Patients with positive serology for HTLV 1 or 2 were excluded. Re-screening for infectious disease markers was not required at baseline (before LD).

Procedures

Study conduct. This trial was conducted in accordance with the Declaration of Helsinki and ICH GCP guidelines. The protocol was approved by local or independent institutional review boards at each trial center (Supplementary Table 13). Written informed consent was obtained from each patient. No compensation was provided for study participation. Participants may have received reimbursement for any costs incurred as a result of study participation. A Safety Review Committee assessed safety signals during dose escalation and adjudicated DLTs. The severity of TEAEs was graded according to National Cancer Institute Common Terminology Criteria for Adverse Events version 5.0. CRS was defined and graded according to criteria developed by Lee et al.¹⁷

Neurologic toxic effects were graded according to Chimeric Antigen Receptor T-cell Therapy-Associated Toxicity 10-point neurological assessment (CARTOX-10) criteria for cell-associated encephalopathy¹⁸.

Screening study (NCT02636855). A screening study was initiated to pre-screen patients ≥ 18 years to ≤ 75 years of age with advanced solid tumors for the presence of inclusion and exclusion alleles (NCT02636855) for referral to this phase 1 trial (NCT03132922). HLA typing was performed using the 510(k)-cleared SeCore high-resolution sequence-based typing system for Class I loci (A, B and C) and uTYPE software (One Lambda Inc., Thermo Fisher Scientific). Central laboratory testing was performed using blood samples at the Histocompatibility/Molecular Genetics Laboratory at the American Red Cross in Philadelphia, Pennsylvania, which is accredited by the American Society for Histocompatibility and Immunogenetics.

For MAGE-A4 antigen expression, centralized testing by IHC was performed at HistoGeneX using an analytically validated and clinical laboratory improvement amendments (CLIA)-certified clinical trial assay. Positivity was determined by a pathologist based on the percentage of positive cells and intensity of expression, as determined by a percent score (P-score) (range, 0–100%) for IHC staining. P-score was defined as stained cell percentage at 1+ intensity + stained cell percentage at 2+ intensity + stained cell percentage at 3+ intensity. During the conduct of patient pre-screening in the expansion group, the study protocol was amended for SS and MRCLS to use a higher cutoff of $\geq 30\%$ of cells that were of 2+ and/or 3+ intensity; a subsequent amendment was made to use this higher cutoff for all other tumor types in the expansion group. For translational data analyses, MAGE-A4 expression was presented as an H-score, which was defined as: (% stained cells at 0) \times 0 + (% stained cells at 1+) \times 1 + (% stained cells at 2+) \times 2 + (% stained cells at 3+) \times 3. The H-score range is 0–300 (refs. 19–21).

Phase 1 study (NCT03132922). Patients who met the pre-screening requirements were then screened for eligibility criteria for this phase 1 trial (NCT03132922), including age ≥ 18 years to ≤ 75 years, ECOG score of 0 or 1, measurable disease per RECIST version 1.1 and adequate organ function, including creatinine clearance (CrCl) ≥ 60 ml min $^{-1}$. Eligible patients entered the interventional phase and then the LTFU phase (Extended Data Fig. 1). Patients who ended the interventional phase continued in the LTFU phase for long-term monitoring for potential gene-therapy-related delayed AEs for 15 years after infusion.

Leukapheresis was performed to obtain CD3 $^{+}$ T cells for afami-cel manufacture. Systemic bridging therapy was permissible before LD chemotherapy.

Patients received LD chemotherapy consisting of fludarabine 30 mg/m 2 and cyclophosphamide 600 mg/m 2 on days -7, -6 and -5 before afami-cel infusion (Supplementary Table 14). Fludarabine doses were adjusted per baseline CrCl: 30 mg/m 2 for patients with CrCl ≥ 80 ml min $^{-1}$ and 20 mg/m 2 for patients with CrCl ≥ 60 ml min $^{-1}$ and < 80 ml min $^{-1}$; patients with CrCl < 60 ml min $^{-1}$ were ineligible for study treatment. Granulocyte colony-stimulating factor could be administered 24 hours after the last fludarabine infusion.

This phase 1 trial was conducted using a 3 + 3 design and involved dose escalation of afami-cel across dose Groups 1–3 and an expansion group. Dose ranges (total transduced cell number) were 0.08×10^9 to 0.12×10^9 cells for Group 1 ($n = 3$, all ovarian cancer); 0.5×10^9 to 1.2×10^9 cells for Group 2 ($n = 3$, all ovarian cancer); 1.2×10^9 to 6.0×10^9 cells for Group 3 ($n = 3$; one esophagogastric junction (EGJ) cancer, one ovarian cancer and one SS); and 1.2×10^9 to 10×10^9 cells for the expansion group ($n = 29$, one EGJ, one esophageal, three head and neck, one melanoma, five MRCLS, two ovarian, 15 SS and two urothelial). Group 1 received LD chemotherapy of cyclophosphamide (600 mg/m 2 /day) on days -7, -6 and -5 and fludarabine (30 mg/m 2 /day) on days -7, -6 and -5. Group 2 received LD chemotherapy of cyclophosphamide (600 mg/m 2 /day) on days -7, -6 and -5 and fludarabine (30 mg/m 2 /day) on days -7, -6

and -5. Group 3 received LD chemotherapy of cyclophosphamide (600 mg/m²/day) on days -7, -6 and -5 and fludarabine (30 mg/m²/day) on days -7, -6, -5 and -4. Most patients in the expansion group ($n=22$) received LD chemotherapy of cyclophosphamide (600 mg/m²/day) on days -7, -6 and -5 and fludarabine (30 mg/m²/day) on days -7, -6, -5 and -4. Seven patients in the expansion group received the higher LD chemotherapy of cyclophosphamide (1,800 mg/m²/day) on days -3 and -2 and in combination with fludarabine (30 mg/m²/day) on days -5, -4, -3 and -2. DLTs were evaluated before each dose escalation, with doses progressively increased to 1.2×10^9 to 10.0×10^9 cells in the expansion group. Eligible patients could receive a second cell infusion after disease progression after a confirmed response.

Evaluation of safety and tolerability was conducted at each study visit as follows: baseline; days -7 to -3; days 1–5; days 8, 15, 22, 29, 36, 43, 57, 71, 85, 127 and 169; every 3 months until year 2; every 6 months from years 2 to 5 or until disease progression; and at completion.

Engineering of afami-cel. Afami-cel was engineered using the Adaptimmune p1.5, p1.5.1 and p1.6.1 manufacturing processes. The p1.5 process used the COBE 2991 Cell Processor cell washer (Terumo BCT) and Xuri Cell Expansion System W25 bioreactor (Cytivia). During the trial, process improvements were made to the volume of material processed, with the process being updated to p1.5.1. Further improvements were made during the trial, with the COBE 2991 Cell Processor being replaced by the Sepax C-Pro Cell Processing System (Cytivia) for the p1.6.1 manufacturing process. Along with changes to the cell manufacturing process over the course of the trial, there were also multiple sources of lentiviral vector. The initial source of vector was manufactured by City of Hope and used an adherent-based manufacturing process. The lentiviral vector sourced later in the trial was manufactured by Lentigen and used a suspension-based manufacturing process. The median vector copy number in the product was 4.5 per transduced cell (range, 2.2–8.5 per transduced cell); the median transduction efficiency for the product was 53.3% (range, 25.5–80%); and the median number of cells produced during the manufacturing process was 20.7×10^9 total nucleated cells (range, 5.0×10^9 to 42.2×10^9). The final cell product release was contingent on several different specifications, including CD3⁺≥80% of cells, vector copy number <12.0 and cell viability ≥70%; the final afami-cel product was cryopreserved in 5% dimethyl sulfoxide and thawed before intravenous administration.

Immunophenotyping and cytotoxicity. Immunophenotypic profiling of MP and PBMC samples was performed by flow cytometry, using multicolor staining panels (CD3 (SK7), CD4 (SK3) and CD8 (SK1), BD Biosciences; CD45RA (H100) and CCR7 (G043H7), BioLegend; and Live/Dead Fix Aqua, Thermo Fisher Scientific). For all samples, in the CD3⁺ live population, subsets of CD4⁺ and CD8⁺ cells (assessed for transduction using a major histocompatibility complex dextramer reagent) were further classified into memory subtypes by expression of CCR7 and CD45RA: central (CM, CD45RA⁻CCR7⁺), effector (EM, CD45RA⁻CCR7⁺), terminally differentiated (EMRA, CD45RA⁺CCR7⁺) and stem cell like (SCM, CD45RA⁺CCR7⁺) (Supplementary Fig. 1). Two-sided paired Wilcoxon test *P* values are shown, linking compared cell types. Immunophenotyping data were collected using BD FACSDiva 9.0 software and analyzed in FlowJo 9.9 (BD). Antibody dilutions are reported in Supplementary Table 15.

Functionality of T cells in samples of MP administered were profiled *in vitro* using an exploratory cellular cytotoxicity assay. Tumor cell growth (A375nucGFP⁺) was tracked using Incucyte image acquisition and analysis (Sartorius). The same control MP sample was profiled in parallel with each sample as a continuity control. Tumor cell growth data were calculated at 72 hours and 125 hours for MP, and degree of tumor cell killing at each timepoint was represented as percentage killing relative to no T cell controls. Cytotoxicity assay data were performed via analysis of collected images within Sartorius Incucyte Zoom software 2019B Rev2.

Cell persistence. Persistence of transduced T cells in PBMCs after infusion was measured using quantitative PCR (qPCR) specific for the packaging signal sequence present in the vector genome. This sequence, absent from the human genome, is integrated in the genome of the transduced host T cell and, thus, acts as a genetic marker specific for transduced cells. Persistence is expressed as the number of vector copies per microgram of genomic DNA from PBMCs.

Lentiviral vector integration site analysis. Lentiviral vector integration sites were identified in DNA extracted from the MPs (transduced T cells) and from PBMC samples collected between 6 months and 15 months after infusion in patients exhibiting high levels of long-term persistence (>1% of transduced PBMCs based on Psi qPCR). The identification and quantification of each integration site was performed using next-generation sequencing using the SonicAbundance method²².

Soluble biomarkers. To evaluate peripheral immune marker profiles, patient-derived serum samples taken before and after afami-cel infusion for the mITT population ($N=38$) were analyzed. Using multiplex assays on the Meso Scale Discovery platform, levels (pg ml⁻¹) of a panel of 22 markers were determined: IFN γ , GM-CSF, TNF- α , TNF- β , vascular endothelial growth factor, IL-1 α , IL-1 β , IL-1RA, IL-2, IL-2R α , IL-4, IL-5, IL-6, IL-7, IL-8, IL-10, IL-12p70, IL-13, IL-15, IL-16, IL-17A and IL-12/IL-23p40. Further exploratory analyses measured 92 immuno-oncology-related human proteins simultaneously using Olink IMMUNO-ONCOLOGY, based on Proximity Extension Assay technology (Olink Bioscience). Detection was performed using the Fluidigm Biomark or the Fluidigm Biomark HD system. Data are reported as Normalized Protein eXpression unit. Data figures were generated using RStudio (and R version 4.2.1) and appropriate R script packages.

Afami-cel RNA *in situ* hybridization and CD3 IHC. RNA *in situ* hybridization for MAGE-A4 coding SPEAR (Advanced Cell Diagnostics) was performed on the Ventana Discovery Ultra automation platform (Roche Diagnostics) using the RNAscope 2.5 LS Red kit (Advanced Cell Diagnostics, 322150) according to the manufacturer's instructions. In brief, 4- μ m formalin-fixed, paraffin-embedded (FFPE) tissue sections were pre-treated with heat and protease before hybridization with the target oligo probes. Pre-amplifier, amplifier and alkaline phosphatase-labeled oligos were then hybridized sequentially. RNAscope assay was followed by CD3 chromogenic precipitate IHC (anti-CD3 (2G6) rabbit monoclonal primary antibody, 790-4341, CONFIRM, Roche Diagnostics) using the DISCOVERY TEAL HRP detection kit (Roche Diagnostics, 08254338001). Each sample was quality controlled for RNA integrity with an RNAscope probe specific to peptidylpropyl isomerase B (PPIB) RNA (Hs-PPIB, 313909). Specific RNA staining signal was identified as red punctate dots, and CD3 was identified by the teal signal. Samples were counterstained with hematoxylin.

The whole slides were scanned using the AxioScan.Z1 microscope slide scanner and analyzed using HALO image analysis software (Indica Labs). Images were annotated and analyzed using Indica Labs ISH version 3.3.9 algorithm, with CD3 staining as the nuclear stain, resulting in CD3⁺ cell count and MAGE-A4 SPEAR percentage positivity.

MAGE-A4 IHC. MAGE-A4 (OriGene, TA505362) IHC staining was performed on 4- μ m sections of FFPE biopsy tissues. Staining was performed and scored at a laboratory certified by the CLIA and accredited by the Belgian Accreditation Organization and College of American Pathologists (HistoGeneX).

Multiplex immunofluorescence staining. Multiplex immunofluorescence staining was performed using Ultivue FixVUE 8-plex multiplex immunostaining kit (CD3, CD4, CD8, FoxP3, granzyme B, Ki67, PanCK/Sox10 and PD-L1) and conducted on a Leica Bond Rx (Leica Biosystems) fully automated immunostainer, according to the kit

protocol. The whole slides were scanned using an AxioScan.Z1 microscope slide scanner; images were stacked using Ultivue's Ultistacker software for InSituPlex image co-registration (version 1.0); and stacked image datasets were analyzed using HALO image analysis software. Images were annotated and analyzed using High Plex FL version 3.2.1 algorithm (Indica Labs), resulting in co-localization output for key immunophenotypes, such as CD4 T cells (CD3⁺CD4⁺), cytotoxic T cells (CD3⁺CD8⁺), regulatory T cells (CD3⁺CD4⁺FoxP3⁺) and malignant cells (PanCK/Sox10⁺) as well as activated (granzyme B⁺), proliferating (Ki67⁺) and PD-L1⁺ combinations of these phenotypes. Spatial analysis plots were generated, using HALO Spatial Analysis module, by selected combinations of these immunophenotypes. The generated spatial plots represent spatial organization and distribution of malignant cells to cytotoxic and regulatory T cells in a selected region of interest. Semi-quantitative analysis of cell numbers (per square millimeter of tumor tissue area), for each of immunophenotype, was performed by exporting the summary results from HALO and importing these data into RStudio (and R version 4.2.1) to generate the relevant heat maps and line plots.

NanoString. FFPE-derived RNA samples were analyzed on the NanoString platform using nCounter PanCancer Immune Profiling Panel (XT-CSO-HIP1-12; NS_CancerImmune_V1.1). Sample quality control was carried out as per the manufacturer's instructions. Background levels were determined for each sample using mean plus two standard deviations of the included negative control counts. Background subtracted counts were normalized using geometric means of 27 housekeeping genes. log₂-normalized counts for the 'T cell exhaustion' gene list was compiled based on published literature²³. 'Negative regulation of T cell-mediated immunity' gene list was obtained from the corresponding Gene Ontology term^{24,25}. Normalized counts were analyzed using the gene set variation analysis algorithm described previously²⁶. Gene lists were extracted from NanoString panel annotation for cell types and immune response categories, excluding any gene list with fewer than three associated genes. Data figures were generated using the ComplexHeatmap R package²⁷. The NanoString data are available publicly at <https://www.ncbi.nlm.nih.gov/geo/query/acc.cgi?acc=GSE202156>.

Outcomes. The primary objective was evaluation of safety and tolerability with endpoints including TEAEs, serious AEs, DLTs and detection of replication-competent lentivirus (RCL). Secondary endpoints included ORR confirmed by RECIST version 1.1, BOR, TTR, DoR, duration of SD, PFS and OS. Exploratory objectives included evaluation of cell persistence and cytokines. Exploratory endpoints included correlation of persistence, phenotype and functionality of transduced (afami-cel) and non-transduced T cells in the peripheral blood and/or tumor in response to treatment and safety; determination of target antigen expression, genes related to antigen processing/presentation and cell surface co-stimulatory ligands; and evaluation of serum cytokines (that is, IL-6). The following exploratory endpoints were not analyzed: evaluation of anti-tumor antibodies or candidate biomarkers from plasma-derived exosomes and cell-free DNA. Owing to the preliminary nature of the data collected before the data cutoff, limited correlative analyses were reported in relation to response to treatment and safety. Two patients received a second infusion; they were non-responders. Therefore, ORR was not evaluated for the second infusion.

Statistical analysis

The sample size for this study was not pre-specified. This phase 1 study was not statistically powered to evaluate either safety or efficacy; hence, the data were summarized descriptively. No formal hypothesis testing was planned. ORR was defined as the proportion of patients with a BOR of confirmed complete response or partial response per

RECIST version 1.1 relative to the total number of patients in the corresponding analysis population. DCR was defined as the percentage of patients whose disease reduced or remained stable as per RECIST version 1.1. PFS, OS, TTR and DoR with 95% CIs were estimated using Kaplan–Meier methods. BOR per RECIST version 1.1 and ORR with 95% CIs were summarized. Censoring of data for DoR and PFS was based on US Food and Drug Administration censoring rules (<https://www.fda.gov/media/71195/download>)^{28,29}. Censoring will occur as follows for DoR:

- If there are no adequate tumor assessments after the patient achieved confirmed response, the DoR will be censored and have a duration set to 1.
- If a patient is known to be alive and progression free, DoR will be censored on the day of the last adequate tumor assessment.
- Use of active curative anti-cancer therapy after T cell infusion (that is, before disease progression) will also be considered as meeting the PD criterion. If a patient is given subsequent curative anti-tumor therapies, curative anti-cancer therapies and curative anti-cancer surgeries other than the study treatment (not including approved palliative radiation and diagnostic procedures, such as surgical biopsies before PD or death), DoR will be censored on the date of the last progression-free tumor assessment before the start date of the anti-tumor treatment.
- If a patient discontinues the interventional phase of the study before PD, DoR will be censored on the date of last adequate progression-free tumor assessment.
- If a patient misses two or more consecutive post-baseline tumor assessments and the following assessment is a PD, or if a patient misses two or more consecutive post-baseline tumor assessments and then dies, DoR will be censored on the date of the last adequate tumor assessment.

Censoring will occur as follows for PFS:

- If a patient has an inadequate baseline scan, PFS will be censored and have a duration set to 1.
- If there are no adequate post-baseline tumor assessments after T cell infusion or date of death recorded, PFS will be censored and have a duration set to 1.
- If a patient is known to be alive and progression free, PFS will be censored on the day of the last adequate tumor assessment.
- To note, use of active curative anti-cancer therapy after T cell infusion (that is, before disease progression) will also be considered as meeting the PD criterion. If a patient is given subsequent curative anti-tumor therapies, curative anti-cancer therapies and curative anti-cancer surgeries other than the study treatment (not including approved palliative radiation and diagnostic procedures, such as surgical biopsies before PD or death), DoR will be censored on the date of the last progression-free tumor assessment before the start date of the anti-tumor treatment.
- If a patient discontinues the interventional phase before PD, PFS will be censored on the date of the last adequate tumor assessment.
- If a patient misses two or more consecutive post-baseline tumor assessments and the following assessment is a PD, or if a patient misses two or more consecutive post-baseline tumor assessments and then dies, PFS will be censored on the date of the last adequate tumor assessment.

Safety data were summarized using descriptive statistics. Persistence of afami-cel, RCL and cytokines were summarized descriptively. Analyses were performed with SAS software version 9.4.

Reporting summary

Further information on research design is available in the Nature Portfolio Reporting Summary linked to this article.

Data availability

The NanoString data are available publicly at <https://www.ncbi.nlm.nih.gov/geo/query/acc.cgi?acc=GSE202156>. The clinical datasets generated and/or analyzed during the current study are available upon reasonable request from the corresponding author for research only, non-commercial purposes. Such datasets include study protocol, statistical analysis plan, individual participant data that underlie the results reported in this article after de-identification (text, tables, figures and appendices) as well as supporting documentation as required. Restrictions relating to patient confidentiality and consent will be maintained by aggregating and anonymizing identifiable patient data. The clinical data will be available beginning immediately after article publication and thereafter with no time limit. Requests should be sent in writing describing the nature of the proposed research and extent of data requirements. Data recipients are required to enter a formal data-sharing agreement that describes the conditions for release and requirements for data transfer, storage, archiving, publication and intellectual property. Requests should be directed to Dennis Williams and will be reviewed by the corresponding senior authors, D.S.H. and M.O.B., and by Adaptimmune. Responses will typically be provided within 60 days of the initial request.

References

17. Lee, D. W. et al. ASTCT consensus grading for cytokine release syndrome and neurologic toxicity associated with immune effector cells. *Biol. Blood Marrow Transplant.* **25**, 625–638 (2019).
18. Neelapu, S. S. et al. Chimeric antigen receptor T-cell therapy—assessment and management of toxicities. *Nat. Rev. Clin. Oncol.* **15**, 47–62 (2018).
19. McCarty, K. S. et al. Estrogen receptor analyses. Correlation of biochemical and immunohistochemical methods using monoclonal antireceptor antibodies. *Arch. Pathol. Lab. Med.* **109**, 716–721 (1985).
20. Parris, T. Z. et al. Clinical relevance of breast cancer-related genes as potential biomarkers for oral squamous cell carcinoma. *BMC Cancer* **14**, 324 (2014).
21. Fedchenko, N. & Reifenrath, J. Different approaches for interpretation and reporting of immunohistochemistry analysis results in the bone tissue—a review. *Diagn. Pathol.* **9**, 221 (2014).
22. Sherman, E. et al. INSPIRED: a pipeline for quantitative analysis of sites of new DNA integration in cellular genomes. *Mol. Ther.* **4**, 39–49 (2017).
23. Wherry, E. & Kurachi, M. Molecular and cellular insights into T cell exhaustion. *Nat. Rev. Immunol.* **15**, 486–499 (2015).
24. Ashburner, M. et al. Gene ontology: tool for the unification of biology. The Gene Ontology Consortium. *Nat. Genet.* **25**, 25–29 (2000).
25. Gene Ontology Consortium. The Gene Ontology resource: enriching a GOld mine. *Nucleic Acids Res.* **49**, D325–D334 (2021).
26. Hänelmann, S., Castelo, R. & Guinney, J. GSVA: gene set variation analysis for microarray and RNA-seq data. *BMC Bioinformatics* **14**, 7 (2013).
27. Gu, Z., Eils, R. & Schlesner, M. Complex heatmaps reveal patterns and correlations in multidimensional genomic data. *Bioinformatics* **32**, 2847–2849 (2016).
28. US Food and Drug Administration. Clinical trial endpoints for the approval of non-small cell lung cancer drugs and biologics guidance for industry. <https://www.fda.gov/media/116860/download> (2015).
29. US Food and Drug Administration. Clinical trial endpoints for the approval of cancer drugs and biologics guidance for industry. <https://www.fda.gov/media/71195/download> (2018).

Acknowledgements

This study was sponsored by Adaptimmune. MD Anderson is supported, in part, by a Cancer Prevention Research Institute of Texas Precision Oncology Decision Support Core Grant (RP150535; D.S.H.); a Comprehensive Cancer Center Core Grant (P30 CA016672; D.S.H.); an MD Anderson Cancer Center Support Grant (NIH/NCI P30 CA016672; D.S.H.); and Clinical Translational Science Award 1UL1 TR003167 (D.S.H.). We thank the participating centers, including The University of Texas MD Anderson Cancer Center; Princess Margaret Cancer Centre; Washington University School of Medicine; Fox Chase Cancer Center; James Cancer Hospital and Solove Research Institute; Sarah Cannon Research Institute; Roswell Park Cancer Institute; Duke University Medical Cancer Center; H. Lee Moffitt Cancer and Research Center; and Sylvester Comprehensive Cancer Center, as well as the patients and their families who participated in this trial. We also thank R. Govindan, Washington University School of Medicine, for work on the screening protocol; A. C. Porter of Syncrogenix, a Certara Company, for medical writing and editorial assistance (financially supported by Adaptimmune); and Amy Ninetto, Scientific Editor, and Erica Goodoff, Senior Scientific Editor, The University of Texas MD Anderson Cancer Center, for editorial assistance.

Author contributions

C.M., D.S.H., E.V.W., J.-M.N., J.P.S., K.O., P.M.F., Q.L., T.T., D.W. and M.O.B. contributed to conceptualization of the trial. D.S.H., E.V.W., J.-M.N., Q.L., T.T., A.J.O., A.J.T., A.S., M.L.J., R.B., T.A., R.W., N.B., M.I., D.G.B., S.R., M.D. and P.M. contributed to data curation. D.S.H., T.T., A.S., R.B., R.W., C.M., J.B., L.F., T.A., N.B., M.I., R.N., F.D.B., J.K.E. and S.B. contributed to formal data analysis. D.S.H. acquired funding for the trial. D.S.H., R.B., C.M., S.B., J.-M.N., Q.L., A.J.O., A.J.T., M.L.J., P.M., P.M.F., M.O.B., A.C., A.G., B.V.T., D.A.L., J.M.C., P.K., G.R.B.J., N.B., G.B., M.I., F.D.B., D.K., D.G.B. and Z.W. participated in the conduct of the research. D.S.H., R.B., Q.L., N.B., M.I., D.G.B. and E.V.W. developed or designed the methodology for the trial. D.S.H., Q.L., E.V.W., C.M., B.V.T., J.M.C., E.E., P.M.F., M.I. and E.N. had management and coordination responsibility for the trial. D.S.H., Q.L., B.V.T., A.J.O., A.J.T., A.C., D.A.L., J.P.S., M.I., R.N., F.D.B. and A.G.M. provided resources for the trial. R.W., F.D.B., J.K.E., D.G.B. and T.A. provided software assistance for the trial. D.S.H., Q.L., B.V.T., A.J.O., A.J.T., E.V.W., C.M., J.M.C., M.L.J. and P.M.F. had oversight and leadership responsibility for the trial. D.S.H., Q.L., R.W., R.B., A.S., T.A., M.I., R.N. and S.R. prepared or created data presentation materials for the manuscript. D.S.H., Q.L., A.S., A.J.O., A.J.T., C.M., M.L.J., J.P.S., S.B., J.-M.N., M.I., R.N. and D.W. were responsible for writing the initial draft. All authors were responsible for reviewing and revising the manuscript.

Competing interests

D.S.H. reports grants and personal fees from Adaptimmune related to this research. Outside the submitted work, D.S.H. reports grants from AbbVie, Adlai Nortye, Bristol Myers Squibb, Daiichi Sankyo, Eisai, Fate Therapeutics, Ignyta, Kite, Kyowa, Loxo Oncology, Merck, MedImmune, Mirati, miRNA, Molecular Templates, Mologen, NCI-CTEP, Novartis, Turning Point Therapeutics, EMD Serono, Erasca, Millenium, Navier, Verastem and VM Oncology; grants and personal fees from Infinity, Pfizer, Seattle Genetics and Numa; grants, personal fees and non-financial support from Amgen, Genentech, Bayer and Takeda; grants and non-financial support from AstraZeneca, Genmab, GlaxoSmithKline and Eli Lilly; non-financial support from AACR, ASCO, Celgene and Philips; personal fees and non-financial support from Janssen; personal fees from Alpha Insights, Axiom, Baxter, Acuta, GLG, Group H, Guidepoint, HCW Precision, Medscape, Merrimack, Prime Oncology, Trieza Therapeutics, WebMD, ST Cube, Tavistock, Boxer Capital, COG and ECOR1 during the conduct of the study; and roles in Molecular Match (advisor), OncoResponse (founder) and Presagia (advisor). B.V.T. reports personal fees, non-financial support and other from Adaptimmune during the conduct of the study related

to this research. Outside the submitted work, B.V.T. reports grants from Pfizer, Merck and Tracon Pharmaceuticals; grants, personal fees, non-financial support and other from GlaxoSmithKline; personal fees from Accuronix Therapeutics, ADRx, Ayala Pharmaceuticals, Cytokinetics, Bayer, Bionest Partners, Intellisphere LLC, Hinshaw & Culbertson LLP, Rodney Law, CRICO Risk Management Foundation and Tracey & Fox Law Firm; having attended advisory board meetings for Apexigen, Daiichi Sankyo, Deciphera Pharmaceuticals, Epizyme, GlaxoSmithKline, Novartis and Eli Lilly; and being a board member for Polaris, outside the submitted work. S.B., C.M., Q.L., A.J.T., J.P.S., R.W., T.T., T.A., S.R., A.S., L.F., J.-M.N., R.B., M.I., R.N., N.B., G.B., Z.W., D.G.B., E.W.W., E.E., P.M.F., E.N. and D.W. report employment by Adaptimmune and stock or stock options in Adaptimmune related to this research. M.L.J. reports grants to the institution from Adaptimmune related to this research. Outside the submitted work, M.L.J. reports grants to the institution from AbbVie, Amgen, Apexigen, Arcus Biosciences, Array BioPharma, Artios Pharma, AstraZeneca, ATRECA, BeiGene, BerGenBio, Birdie Pharmaceuticals/Seven & Eight Biopharmaceuticals, Boehringer Ingelheim, Calithera Biosciences, Checkpoint Therapeutics, Corvus, Cytomx, Daiichi Sankyo, Dracen Pharmaceuticals, Dynavax, EMD Serono, Genentech/Roche, Genmab, Genocea, GlaxoSmithKline, Gritstone Oncology, Harpoon Therapeutics, Hengrui Therapeutics, Immunocore, Incyte, Janssen, Eli Lilly, Loxo Oncology, Lycera, Merck, Mirati Therapeutics, Neovia, Novartis, Pfizer, PMV Pharmaceuticals, Regeneron, Ribon Therapeutics, Sanofi, Shattuck Labs, Silicon Therapeutics, Stemcentrx, Syndax, Takeda, Tarveda Therapeutics, TCR2 Therapeutics, TMUNITY Therapeutics, University of Michigan and WindMIL Therapeutics; other from spouse role as a contract lobbyist for Astellas and Otsuka Pharmaceuticals; and other to the institution from AbbVie, Amgen, AstraZeneca, Boehringer Ingelheim, Bristol Myers Squibb, Calithera Biosciences, Celgene, Daiichi Sankyo, Editas Medicine, Eisai, EMD Serono, G1 Therapeutics, Genentech/Roche, GlaxoSmithKline, Gritstone Oncology, Ideaya Biosciences, Incyte, Janssen, Eli Lilly, Loxo Oncology, Merck, Mirati Therapeutics, Novartis, Pfizer, Ribon Therapeutics, Sanofi and WindMIL Therapeutics. A.J.O. reports non-financial support from Adaptimmune during the conduct of the study related to this research. Outside the submitted work, A.J.O. reports personal fees from Merck, Bristol Myers Squibb, Sanofi, Eisai and Pfizer. J.M.C. reports grants from Adaptimmune related to this study. Outside the submitted work, J.M.C. reports grants from Bristol Myers Squibb, CBMG, Spectrum, Medpacto, Bayer, AbbVie, Moderna, GlaxoSmithKline, Array and CGMB; personal fees from Guardant; grants, personal fees and non-financial support from AstraZeneca, Pfizer, NGM Biopharmaceuticals, Merck and Lung Cancer Initiative of North Carolina; and grants and personal fees from Genentech. D.A., P.K., F.D.B., J.K.E., D.K., A.C., A.G.M. and D.A.L. declare no competing interests. G.R.B.J. reports grants or contracts from Adaptimmune related to this study. Outside the submitted work, G.R.B.J. reports grants or contracts from Amgen, Bayer, Eleelixis, Daiichi Sankyo, GlaxoSmithKline, Immatics, Immunocore, Incyte, Kite Pharma, Macrogenics, Torque, AstraZeneca, Bristol Myers Squibb, Celgene, Genentech, MedImmune, Merck, Novartis, Roche, Sanofi,

Xcovery, Tmunity Therapeutics, Regeneron, BeiGene, Repertoire Immune Medicines, Verastem, CytomX Therapeutics and Duality Biologics; consulting fees from Abbvie, Adicet, Amgen, Ariad, Bayer, Clovis Oncology, AstraZeneca, Bristol Myers Squibb, Celgene, Daiichi Sankyo, Instil Bio, Genentech, Genzyme, Gilead, Eli Lilly, Janssen, MedImmune, Merck, Novartis, Roche, Sanofi, Tyme Oncology, Xcovery, Virogin Biotech, Maverick Therapeutics, BeiGene, Rgeneron, Cytomx Therapeutics, Intervenn Biosciences and Onconova Therapeutics; participation on a Data Safety Monitoring Board or Advisory Board for Virogin Biotech and Maverick Therapeutics; stock or stock options in Virogin Biotech; and other financial or non-financial interests in Johnson & Johnson/Janssen (immediate family member). J.B. works as a contractor for Adaptimmune and contributed to the research reported here. A.G. reports consulting or advisory role for Kite Pharma, Amgen, Atara, Wugen and Celgene; research funding from Kite Pharma, Genentech and Amgen; and honoraria from Kite Pharma, outside the submitted work. Outside the submitted work, P.M. reports personal fees from Bristol Myers Squibb, Celgene, Fate Therapeutics, Janssen, Juno, Karyopharm, Magenta Therapeutics, Oncopeptides and Takeda. M.D. reports personal fees from Adaptimmune related to this research. Outside the submitted work, M.D. reports personal fees from Blueprint and personal fees and non-financial support from Deciphera, Epizyme and Daiichi Sankyo. K.O. reports grants from AstraZeneca and Tessaro outside the submitted work and patent PCT/US2014025673, licensed to Tactiva Therapeutics, and patent PCT/US2014025456, licensed to Tactiva Therapeutics. M.O.B. reports a consulting or advisory role with Adaptimmune related to this research. Outside the submitted work, M.O.B. reports honoraria from Bristol Myers Squibb, Merck, Novartis and Roche; a consulting or advisory role with Bristol Myers Squibb, EMD Serono, Genzyme, GlaxoSmithKline, Immunocore, Immunovaccine, Instil Bio, Iovance Biotherapeutics, LaRoche Posay, Merck, Novartis, Sanofi and Sun Pharma; research funding from Merck and Takara; and expert testimony for Merck.

Additional information

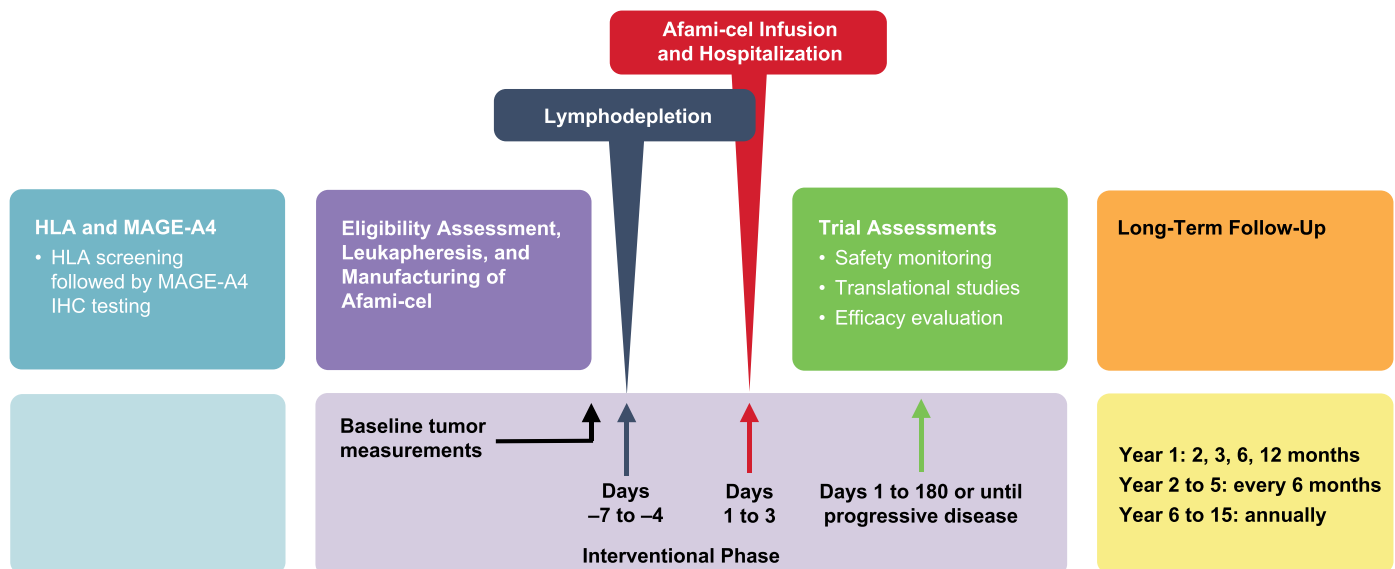
Extended data is available for this paper at <https://doi.org/10.1038/s41591-022-02128-z>.

Supplementary information The online version contains supplementary material available at <https://doi.org/10.1038/s41591-022-02128-z>.

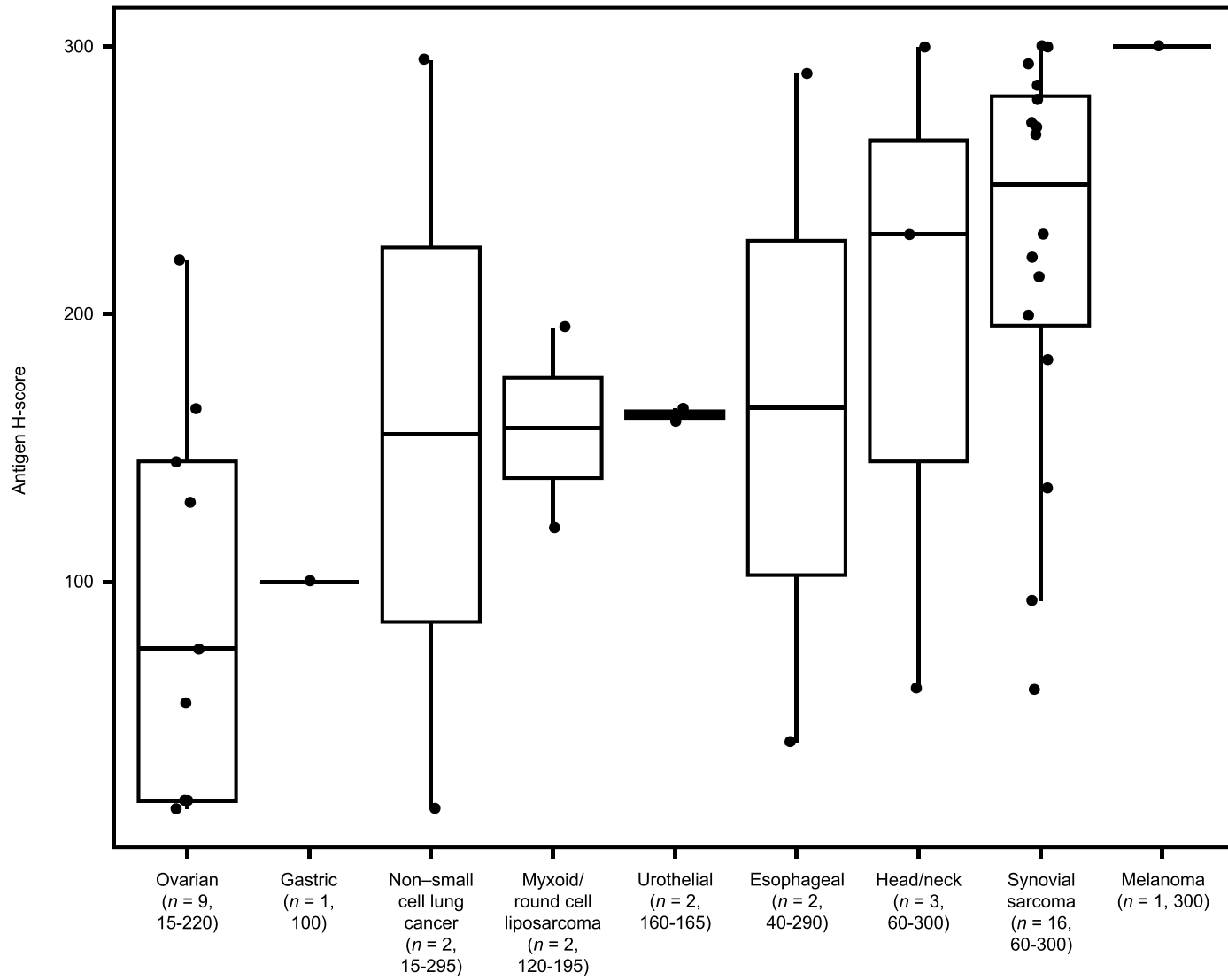
Correspondence and requests for materials should be addressed to David S. Hong.

Peer review information *Nature Medicine* thanks Sebastian Bauer and the other, anonymous, reviewer(s) for their contribution to the peer review of this work. Primary Handling Editors: Saheli Sadanand and Joao Monteiro, in collaboration with the *Nature Medicine* team.

Reprints and permissions information is available at www.nature.com/reprints.

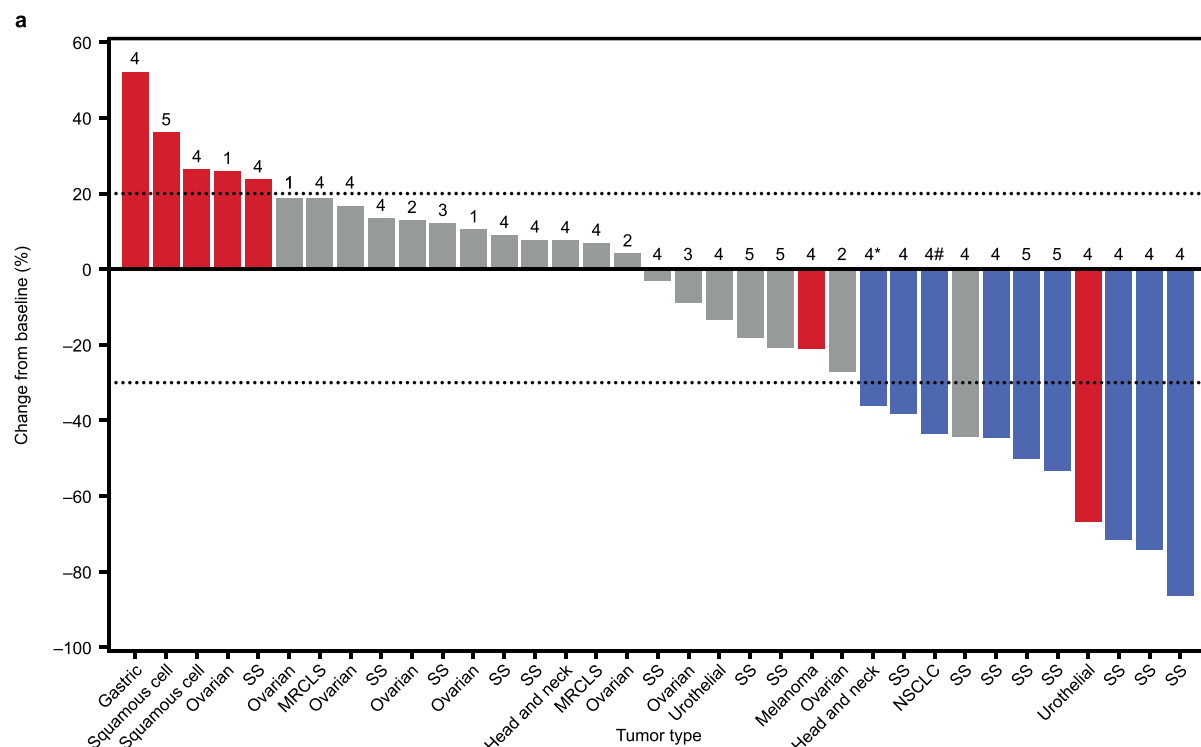


Extended Data Fig. 1 | Study design. HLA, human leukocyte antigen; IHC, immunohistochemistry; MAGE-A4, melanoma-associated antigen A4.



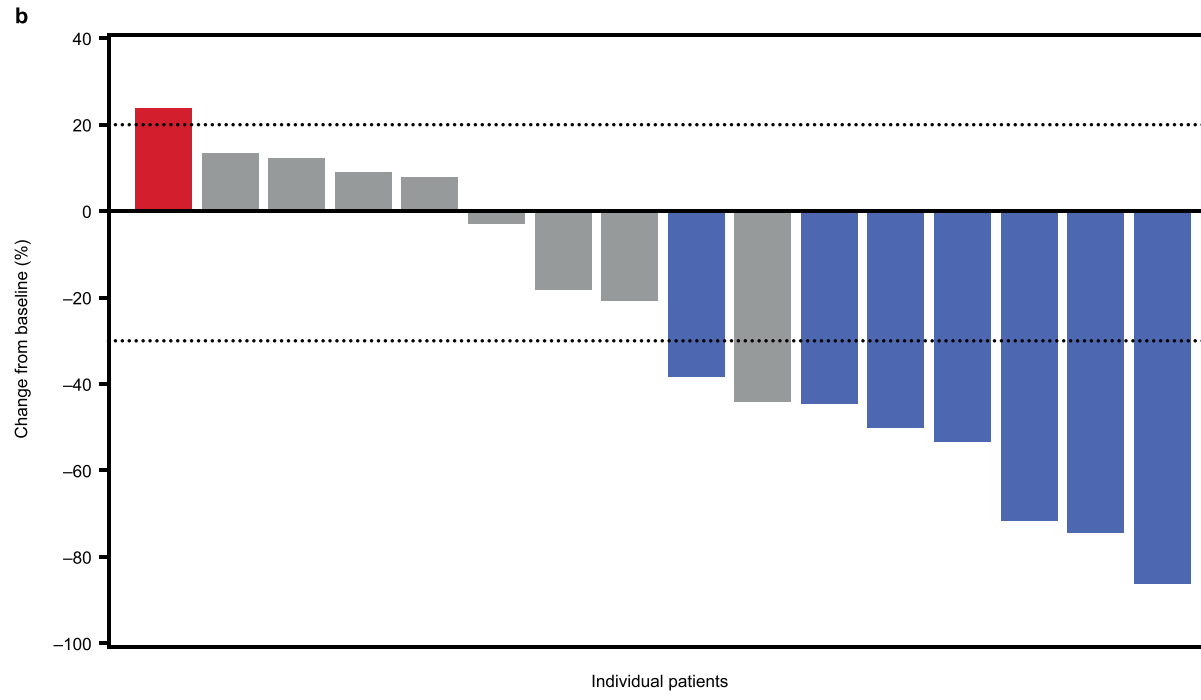
Extended Data Fig. 2 | MAGE-A4 antigen H-score in the modified intent-to-treat population by tumor type. Individual MAGE-A4 antigen H-scores per tumor type. The overall median MAGE-A4 H-score across all nine tumor types was 189 (range: 15–300). Median MAGE-A4 H-score was highest at 249 in synovial sarcoma (range: 60–300); melanoma sub-group excluded due to a single evaluable patient. Box plots depict median as horizontal lines within

boxes, with box bounds as the first and third quartiles. Dots represent individual data points. Lower whisker is the minimum value of the data within 1.5 times the interquartile range below the 25th percentile. Upper whisker is the maximum value of the data within 1.5 times the interquartile range above the 75th percentile. MAGE-A4, melanoma-associated antigen A4.



1. **Group 1:** Cyclophosphamide (600 mg/m²/day) on Days -7, -6, and -5; fludarabine (30 mg/m²/day) on Days -7, -6, and -5
2. **Group 2:** Cyclophosphamide (600 mg/m²/day) on Days -7, -6, and -5; fludarabine (30 mg/m²/day) on Days -7, -6, and -5
3. **Group 3:** Cyclophosphamide (600 mg/m²/day) on Days -7, -6, and -5; fludarabine (30 mg/m²/day) on Days -7, -6, -5, and -4
4. **Expansion:** Cyclophosphamide (600 mg/m²/day) on Days -7, -6, and -5; fludarabine (30 mg/m²/day) on Days -7, -6, -5, and -4
5. **Expansion:** Cyclophosphamide (1,800 mg/m²/day) for Days -3, -2 in combination with fludarabine (30 mg/m²/day) on Days -5, -4, -3, -2
Afami-cel doses: Dose groups 1, 2, and 3 (3 patients each) were treated with medians of 0.1×10^9 cells, 1.2×10^9 cells, and 5.67×10^9 cells, respectively. The expansion group (29 patients) and dose group 3 + expansion group (32 patients) were treated with medians of 7.85×10^9 cells and 7.65×10^9 cells, respectively

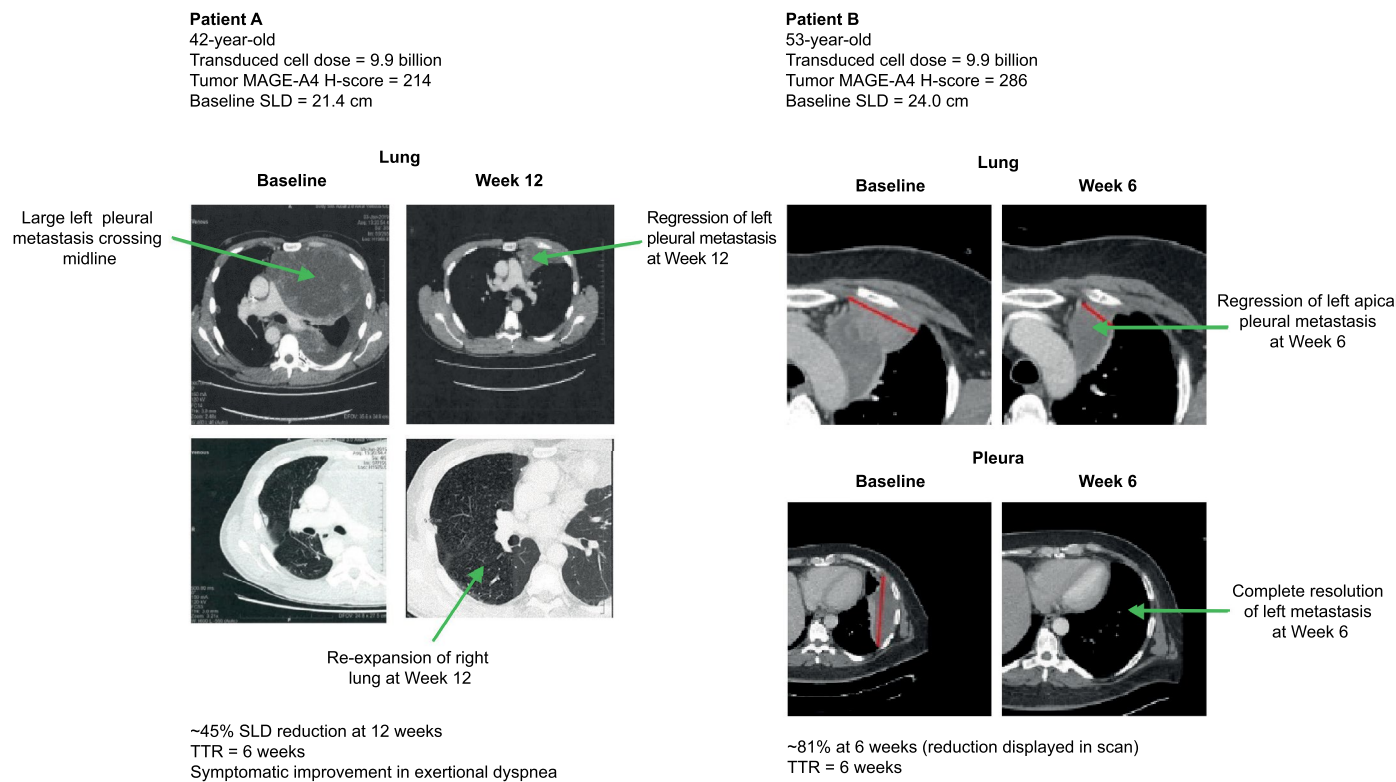
All patients with partial response were patients with SS, except for 1 patient with head and neck* cancer and 1 patient with NSCLC#



Extended Data Fig. 3 | See next page for caption.

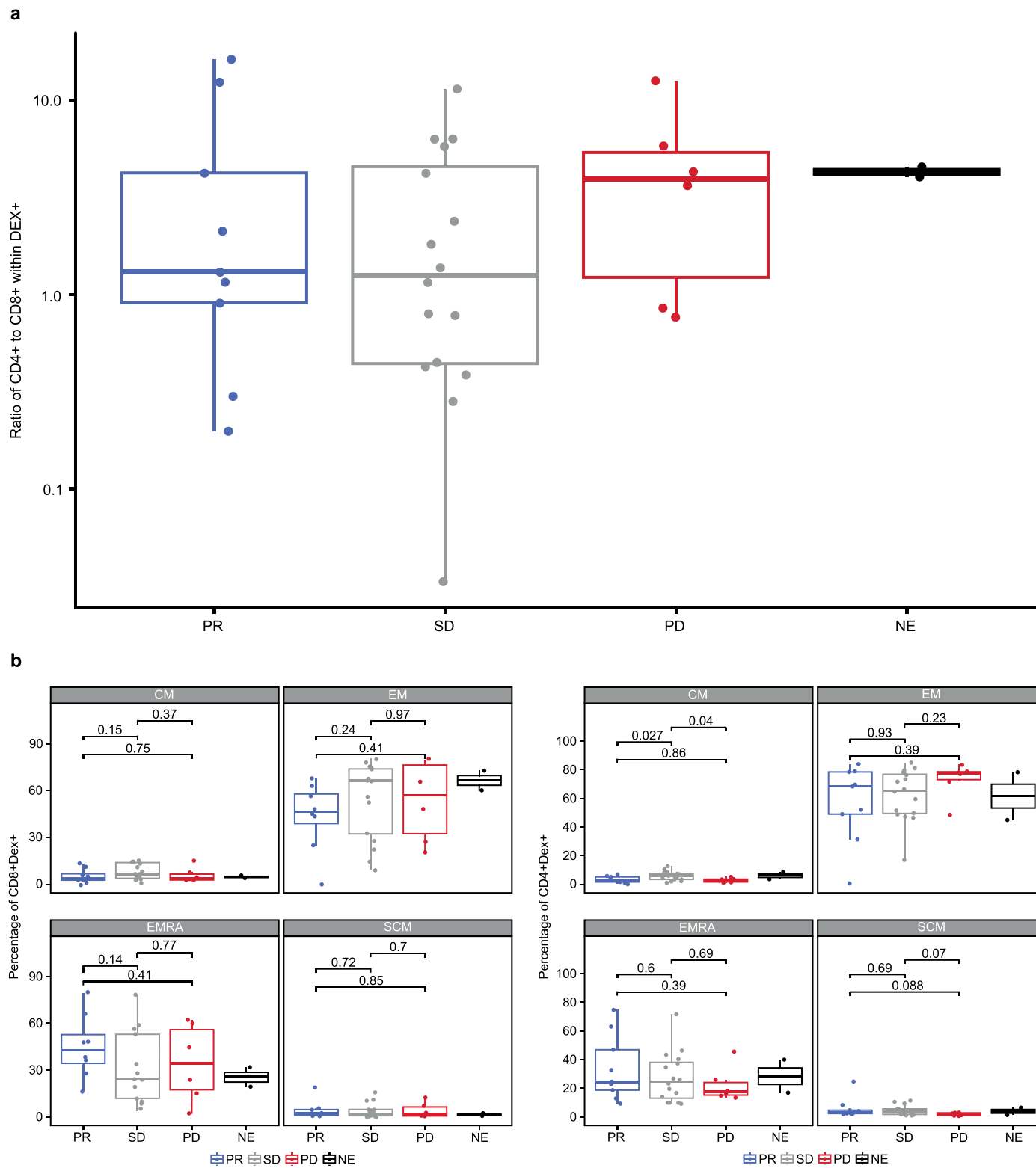
Extended Data Fig. 3 | Maximal change in target lesion from baseline using RECIST v1.1 (modified intent-to-treat population; $N = 38$). (a) Maximal change in target lesion from baseline in the modified intent-to-treat population. Data for three patients were not available as of data cut-off on 1 September 2020. Each bar represents an individual patient. Nine patients responded to first infusion as determined by RECIST v1.1 criteria. All nine responders (23.7%) had a partial response with an overall response rate of 23.7% (95% CI: 11.4, 40.2). (b)

Synovial sarcoma subgroup: Maximal change in target lesion from baseline in the synovial sarcoma subgroup. Each bar represents an individual patient. Seven of the nine responders were in the synovial sarcoma subgroup ($n = 16$) with a best overall response of partial response and an overall response rate of 43.8% (95% CI: 19.8, 70.1). Horizontal reference lines at -30% and 20%. CI, confidence interval; MRCLS, myxoid/round cell liposarcoma; NSCLS, non-small cell lung cancer; RECIST, Response Evaluation Criteria in Solid Tumors; SS, synovial sarcoma.



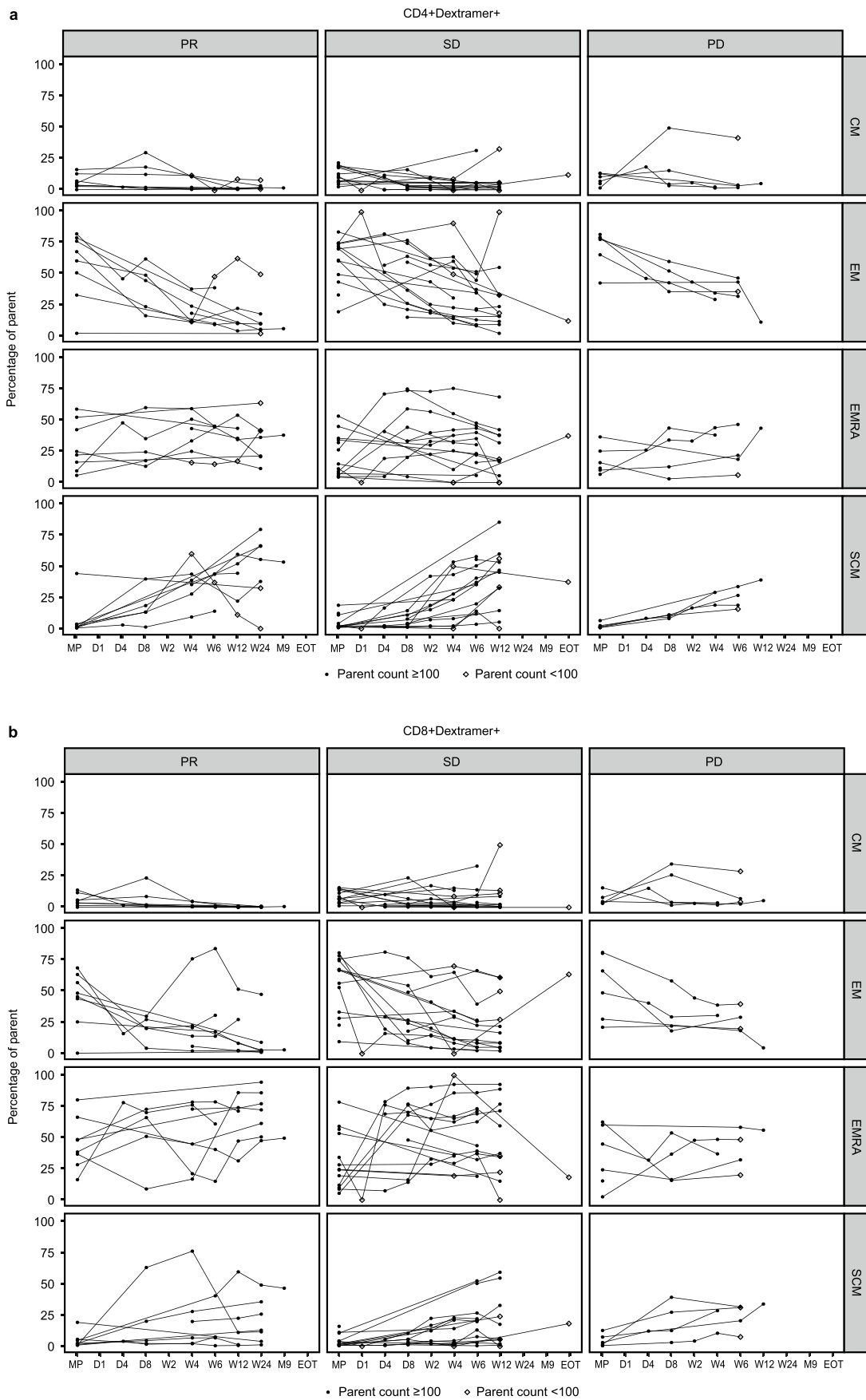
Extended Data Fig. 4 | Afami-cel therapy leads to regression of large pleural-based thoracic metastasis in synovial sarcoma. In Patient A, afami-cel was associated with reductions in metastatic disease in hemithorax, including regression of a large left lung pleural metastasis that crossed the midline at baseline (Patient A, upper right and upper left panels, respectively) and re-expansion of the right lung, as shown on a computed tomography scan at

Week 12 post-afami-cel (Patient A, lower right panel, arrow), associated with patient-reported improvement in exertional dyspnea. In Patient B, afami-cel was associated with overall reduction in left lung pleural metastases including complete resolution of one pleural metastasis (Patient B, lower right panel, arrow). BOR, best overall response; MAGE-A4, melanoma-associated antigen A4; PR, partial response; SLD, sum of longest diameter; TTR, time to response.



Extended Data Fig. 5 | Ratio of transduced CD4⁺ to CD8⁺ cells and memory sub-populations in afami-cel manufactured product. (a) Ratio of CD4⁺ to CD8⁺ cell subsets within the transduced cells infused, derived from immunophenotyping: Ratios greater than 1 denote a CD4 bias in the transduced cells. Horizontal lines denote median values. Samples are grouped and color coded by BOR resulting from the infusion (blue PR, gray SD, red PD, black NE). Ratio of PR range 0.19–16.16 (median 1.30, $n = 9$) vs. SD range 0.03–11.58 (median 1.26, $n = 16$) vs. PD range 0.76–12.52 (median 3.94, $n = 6$). (b) Memory subset distribution by immunophenotyping within the transduced cells infused: The proportion of live single transduced afami-cel within the respective memory subsets is indicated by box plots for CD8⁺ afami-cel on the left and

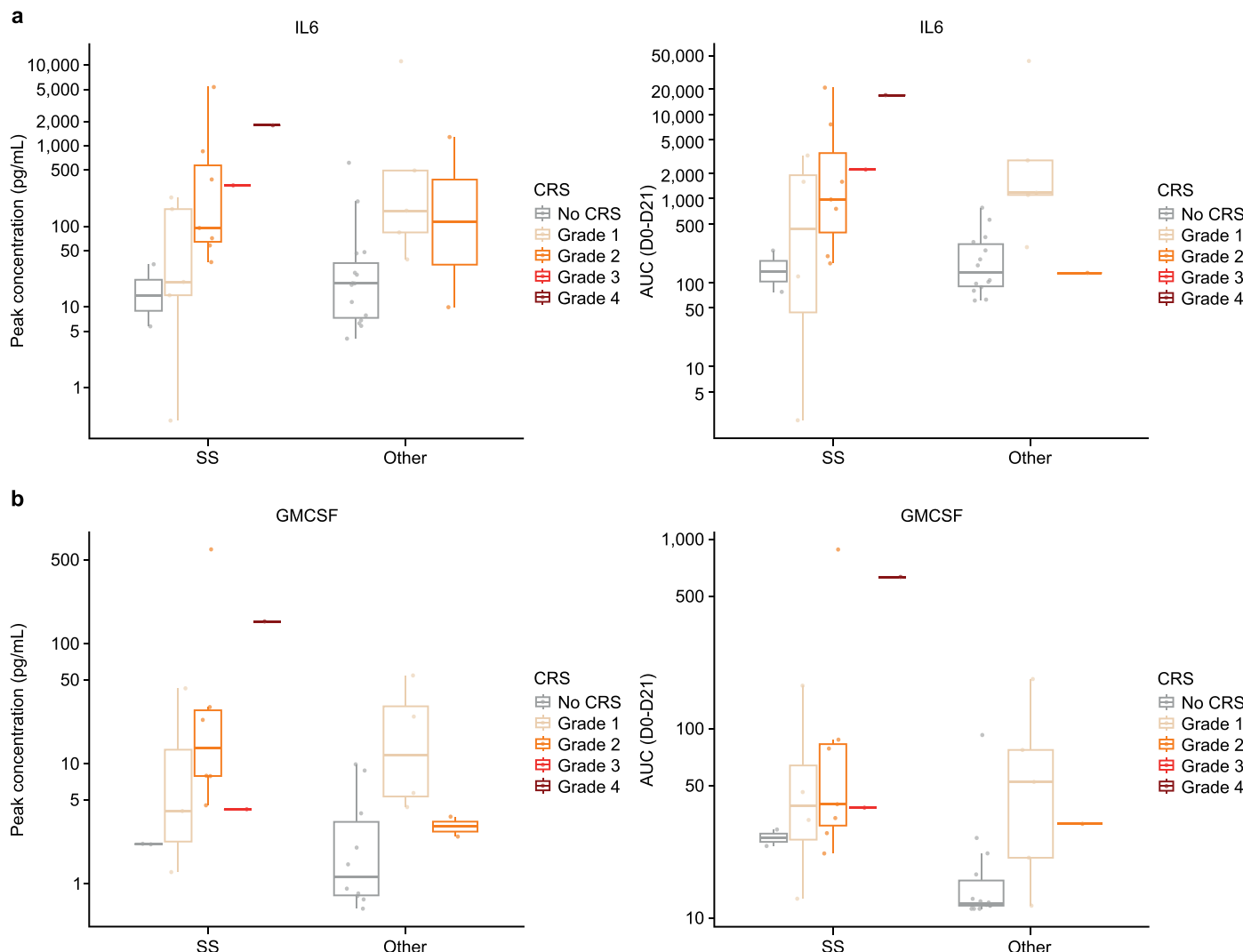
for CD4⁺ on the right. Samples are grouped and color coded by BOR resulting from the infusion (blue PR, gray SD, red PD, black NE). CM = central memory, CD45RA⁺CCR7⁺; EM = effector memory, CD45RA⁺CCR7⁺; EMRA = effector memory RA⁺, CD45RA⁺CCR7⁺; SCM = stem cell memory, CD45RA⁺CCR7⁺. Two-sided paired Wilcoxon test P values are shown linking compared cell types. Box plots depict median as horizontal lines within boxes, with box bounds as the first and third quartiles. Dots represent individual data points. Lower whisker is the minimum value of the data within 1.5 times the interquartile range below the 25th percentile. Upper whisker is the maximum value of the data within 1.5 times the interquartile range above the 75th percentile. BOR, best overall response; DEX, dextramer; NE, not evaluable; PD, progressive disease; PR, partial response; SD, stable disease.



Extended Data Fig. 6 | See next page for caption.

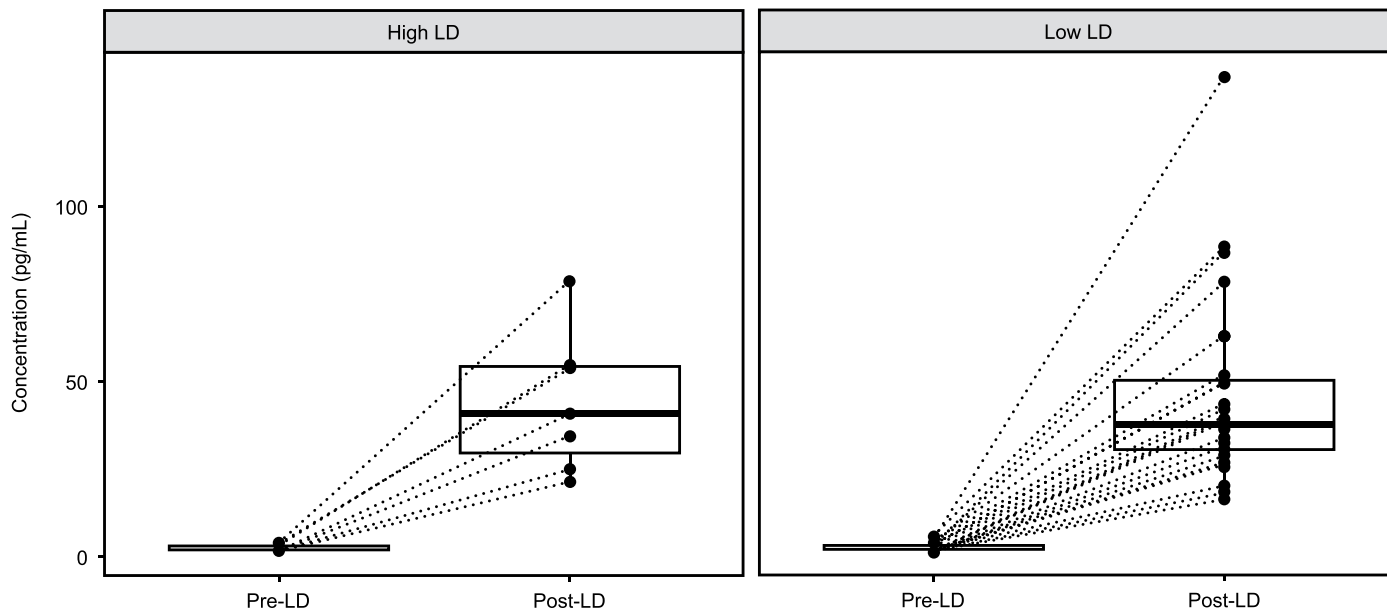
Extended Data Fig. 6 | Longitudinal immunophenotyping of memory subtypes within circulating afami-cel. Percentage of parent population (a) CD4⁺ Dextramer⁺ and (b) CD8⁺ Dextramer⁺ within the respective sub-population flow gate in MP (manufactured product) and peripheral blood mononuclear cell samples at post-infusion timepoints (D, day; W, week; M, month, EOT, end of

treatment). CM (central memory CD45RA⁻CCR7⁺); EM (effector memory CD45RA⁻CCR7⁻); EMRA (effector memory RA⁺, CD45RA⁻CCR7⁻); SCM (stem cell memory, CD45RA⁺CCR7⁻). Data are grouped by best overall response resulting from the infusion. PR (partial response), $n = 9$ patients; SD (stable disease), $n = 17$ patients; PD (progressive disease), $n = 6$ patients.



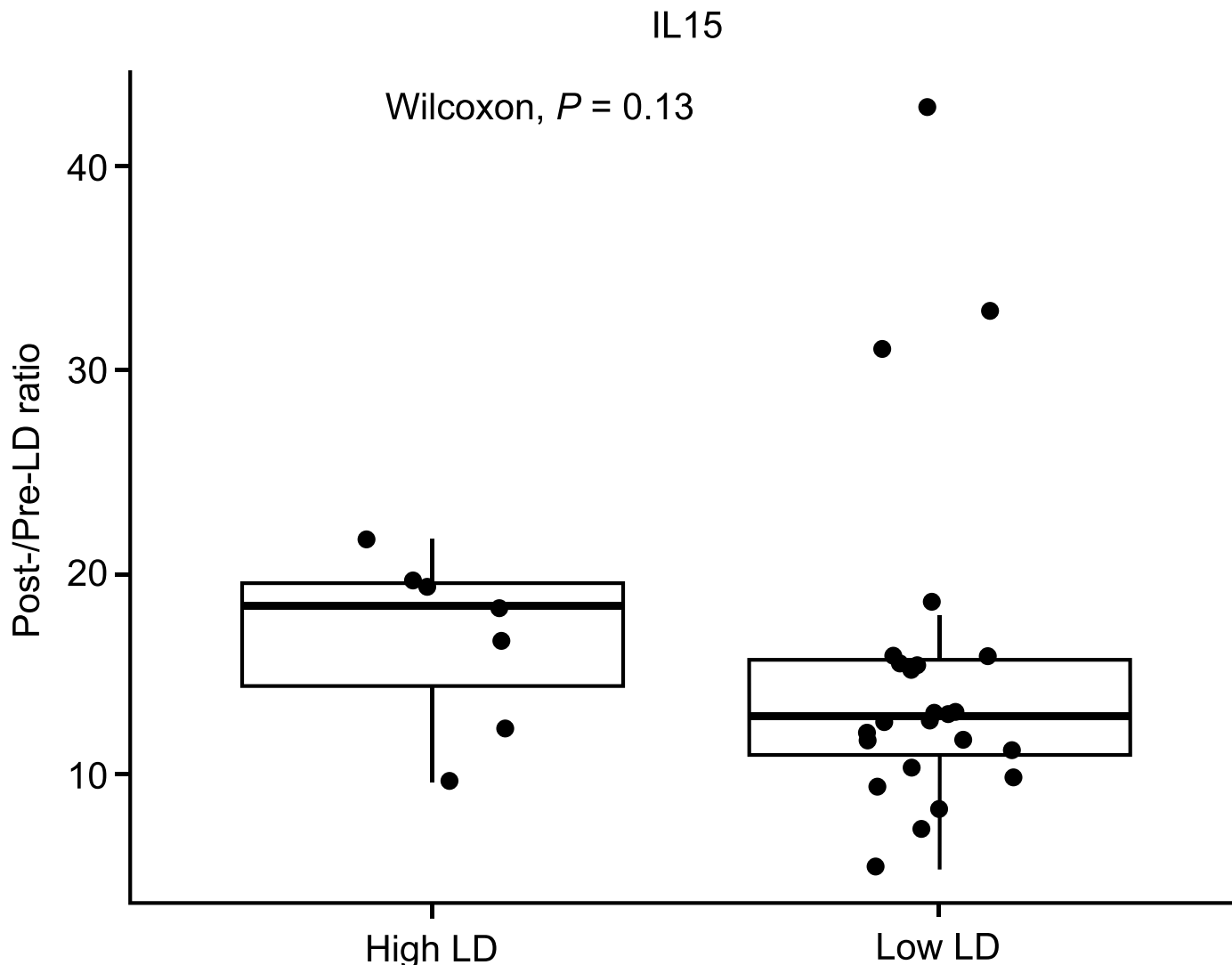
Extended Data Fig. 7 | Serum cytokine profiles associated with cytokine release syndrome. Peak IL-6 levels pg mL^{-1} (a, left panel), calculated IL-6 AUC Day 0–21 (a, right panel), peak GMCSF levels pg mL^{-1} (b, left panel) and calculated GMCSF AUC Day 0–21 (b, right panel) were significantly greater in patients with CRS (all grades, $n = 21$) compared with non-CRS ($n = 17$) in the mITT population (Supplementary Table 8). Box plots show comparison of serum levels in SS patients (no CRS $n = 2$, Grade 1 $n = 5$, Grade 2 $n = 7$, Grade 3 $n = 1$, Grade 4 $n = 1$) and those with other indications (no CRS $n = 15$, Grade 1 $n = 5$, Grade 2 $n = 2$) across

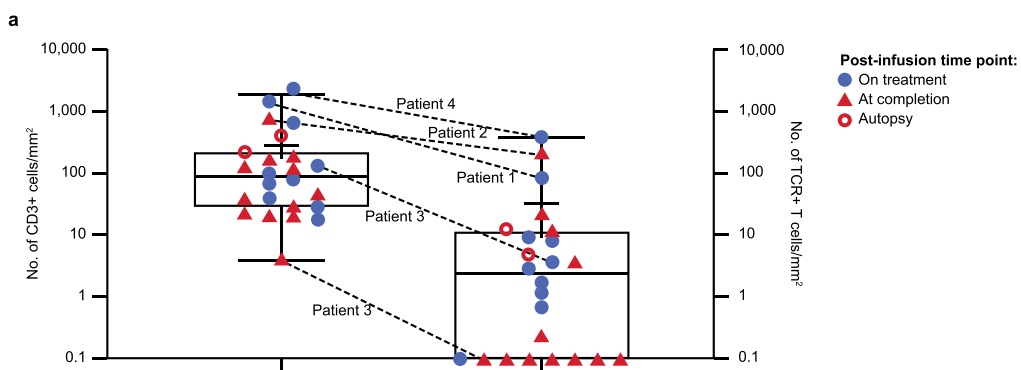
CRS groups. Box plots depict median as horizontal lines within boxes, with box bounds as the first and third quartiles. Dots represent individual data points. Lower whisker is the minimum value of the data within 1.5 times the interquartile range below the 25th percentile. Upper whisker is the maximum value of the data within 1.5 times the interquartile range above the 75th percentile. AUC, area under the curve; CRS, cytokine release syndrome; GMCSF, granulocyte-macrophage colony-stimulating factor; IL, interleukin; SS, synovial sarcoma.



Extended Data Fig. 8 | IL-15 serum concentrations in patients treated with high dose (3600 mg/m²) or low dose (1800 mg/m²) lymphodepleting chemotherapy pre- and post-lymphodepletion. Serum IL-15 levels pg ml⁻¹ were measured pre- and post-LD in Group 3/Expansion patients treated with 'high' LD ($n = 7$) or 'low' LD ($n = 24^*$) regimen (*excludes one patient with an unevaluable baseline sample). Box plots depict median as horizontal lines within boxes, with

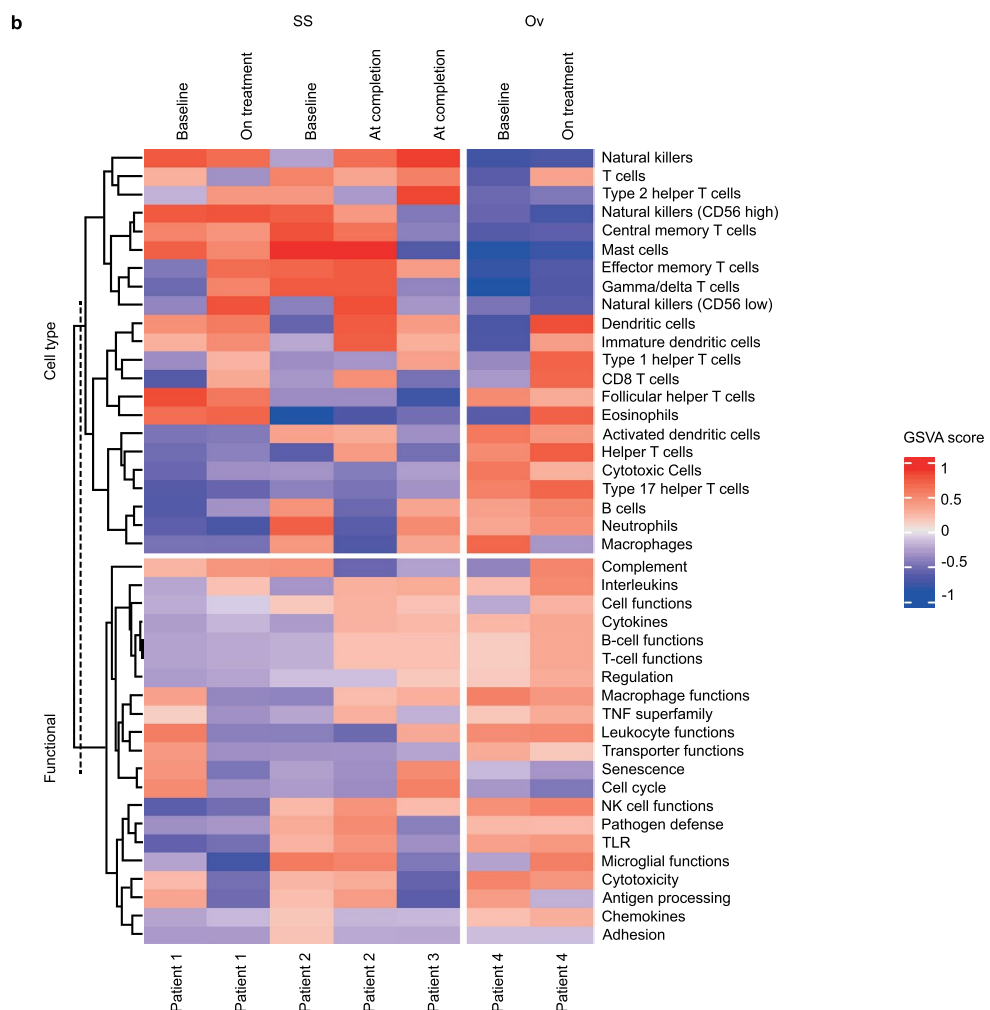
box bounds as the first and third quartiles. Dots represent individual data points. Lower whisker is the minimum value of the data within 1.5 times the interquartile range below the 25th percentile. Upper whisker is the maximum value of the data within 1.5 times the interquartile range above the 75th percentile. IL, interleukin; LD, lymphodepletion.





	Pt 1 (SS)	Pt 2 (SS)	Pt 3 (SS) (CT scan Pt A)	Pt 4 (ovarian cancer)
MAGE-A4 H-Score	300	200	214	220
Target Lesion Baseline SLD (cm)	15.5	4.3	21.4	4.2
Transduced Cell Dose	9.9×10^9	9.9×10^9	9.9×10^9	9.4×10^9
BOR (SLD reduction %)	PR (-72%)	SD (-47%)	PR (-45%)	SD (+17%)
Cell Persistence C_{max} (number of transduced cells/ μ L)	291	830	105	291
Cell Persistence AUC₀₋₂₈ (number of transduced cells*day/ μ L)	2005	16998	1741	5576
Serum IFN-γ C_{max} (pg/nL)	38849	158	4524	121

AUC₀₋₂₈, area under the concentration time curve from Day 0 to Day 28; BOR, best overall response; cm, centimeter; C_{max}, maximum concentration; CT, computed tomography; MAGE-A4, melanoma-associated antigen A4; PR, partial response; Pt, patient; SD, stable disease; SLD, sum of the longest diameter; SS, synovial sarcoma



Extended Data Fig. 10 | See next page for caption.

Extended Data Fig. 10 | Detection of afami-cel and characterization of phenotypes in patient tumor biopsies. (a) Quantification of CD3⁺ T cells and afami-cel in post-infusion tumor biopsies from dose expansion: Four patients with contrasting profiles were prioritized for multiplex immunofluorescence analyses (summarized in Fig. 4a). Patient 1, SS, on-treatment biopsy taken 8 weeks post-infusion; Patient 2, SS, at completion biopsy taken 17 weeks post-infusion; Patient 3, SS, on-treatment and at-completion biopsies taken 7 and 25 weeks post-infusion, respectively; Patient 4, Ov tumor, on-treatment biopsy taken 6 weeks post-infusion. Table summarizes key baseline tumor characteristics, afami-cel dose, post-infusion pharmacokinetic-pharmacodynamic findings, and BOR status for these four patients. Patients 1-3 were patients with SS; Patient 4 was a patient with Ov cancer. Box plots depict median as horizontal lines within

boxes, with box bounds as the first and third quartiles. Dots represent individual data points. Lower whisker is the minimum value of the data within 1.5 times the interquartile range below the 25th percentile. Upper whisker is the maximum value of the data within 1.5 times the interquartile range above the 75th percentile. (b) Heatmap of GSVA scores of cell type specific and immune response categories gene lists in baseline and post-infusion biopsies from Patients 1–4. AUC, area under the curve; BOR, best overall response; C_{max}, maximum serum concentration; CT, computed tomography; GSVA, gene set variation analysis; IFN, interferon; MAGE-A4, melanoma-associated antigen A4; NK, natural killer; Ov, ovarian; PR, partial response; Pt, patient; SD, stable disease; SLD, sum of longest diameter; SS, synovial sarcoma; TCR, T-cell receptor; TLR, toll-like receptor; TNF, tumor necrosis factor.

Reporting Summary

Nature Portfolio wishes to improve the reproducibility of the work that we publish. This form provides structure for consistency and transparency in reporting. For further information on Nature Portfolio policies, see our [Editorial Policies](#) and the [Editorial Policy Checklist](#).

Statistics

For all statistical analyses, confirm that the following items are present in the figure legend, table legend, main text, or Methods section.

n/a Confirmed

- The exact sample size (n) for each experimental group/condition, given as a discrete number and unit of measurement
- A statement on whether measurements were taken from distinct samples or whether the same sample was measured repeatedly
- The statistical test(s) used AND whether they are one- or two-sided
Only common tests should be described solely by name; describe more complex techniques in the Methods section.
- A description of all covariates tested
- A description of any assumptions or corrections, such as tests of normality and adjustment for multiple comparisons
- A full description of the statistical parameters including central tendency (e.g. means) or other basic estimates (e.g. regression coefficient) AND variation (e.g. standard deviation) or associated estimates of uncertainty (e.g. confidence intervals)
- For null hypothesis testing, the test statistic (e.g. F , t , r) with confidence intervals, effect sizes, degrees of freedom and P value noted
Give P values as exact values whenever suitable.
- For Bayesian analysis, information on the choice of priors and Markov chain Monte Carlo settings
- For hierarchical and complex designs, identification of the appropriate level for tests and full reporting of outcomes
- Estimates of effect sizes (e.g. Cohen's d , Pearson's r), indicating how they were calculated

Our web collection on [statistics for biologists](#) contains articles on many of the points above.

Software and code

Policy information about [availability of computer code](#)

Data collection BD FACSDiva 9.0; Sartorius Incucyte Zoom software 2019B Rev2; MSD SQ120 reader; Fluidigm® Biomark™ system; Indica Labs HALO® image analysis software.

Data analysis SAS version 9.4; BD FlowJo 9.9; Sartorius Incucyte Zoom software 2019B Rev2; Indica Labs HALO® image analysis software and ISH version 3.3.9 algorithm; R-studio (and R-4.2.1 version), ComplexHeatmap and appropriate R script packages.

For manuscripts utilizing custom algorithms or software that are central to the research but not yet described in published literature, software must be made available to editors and reviewers. We strongly encourage code deposition in a community repository (e.g. GitHub). See the Nature Portfolio [guidelines for submitting code & software](#) for further information.

Data

Policy information about [availability of data](#)

All manuscripts must include a [data availability statement](#). This statement should provide the following information, where applicable:

- Accession codes, unique identifiers, or web links for publicly available datasets
- A description of any restrictions on data availability
- For clinical datasets or third party data, please ensure that the statement adheres to our [policy](#)

The NanoString data are available publicly at: <https://www.ncbi.nlm.nih.gov/geo/query/acc.cgi?acc=GSE202156>. The clinical datasets generated during and/or analyzed during the current study are available upon request from the corresponding author for research only, non-commercial purposes. Such datasets include

study protocol, SAP, individual participant data that underlie the results reported in this article after de-identification (text, tables, figures and appendices), as well as supporting documentation as required. Restrictions relating to patient confidentiality and consent will be maintained by aggregating and anonymizing identifiable patient data. The clinical data will be available beginning immediately following article publication and thereafter with no time limit. Requests should be sent in writing describing the nature of the proposed research and extent of data requirements. Data recipients are required to enter a formal data sharing agreement that describes the conditions for release and requirements for data transfer, storage, archiving, publication and intellectual property. Requests should be directed to Dennis Williams, PharmD, and will be reviewed by the corresponding senior authors DSH and MOB, and by Adaptimmune. Responses will typically be provided within 60 days of the initial request.

Human research participants

Policy information about [studies involving human research participants and Sex and Gender in Research](#).

Reporting on sex and gender

This first-in-human study included a 3+3 dose-escalation scheme designed to understand the optimal dose among patients, with biological characteristics such as age, weight, and sex inherently considered due to the nature of the study. Representatives of both sexes (male n=22, 57.9%; female, n=16, 42.1%) were included in the trial (reported in Table 1). Sex was determined based on self-reporting; patients were asked to check a box indicating their biological sex with only two options (ie., male or female). Gender information was not collected. No sex-based analyses were performed as there were no apparent differences in optimal dose or safety between males and females.

Population characteristics

Population demographics are reported in Table 1 and Supplementary Table 2. A brief summary is as follows: adult patients, aged 18-75 with advanced solid cancers across 9 tumor types, previously treated with SOC agents, Eastern Cooperative Oncology Group (ECOG) score of 0 or 1, measurable disease per RECIST v1.1, adequate organ function including creatinine clearance ≥ 60 ml/min, and HLA-A*02 positive with tumor. expression of MAGE-A4 antigen. As mentioned below, covariates were not controlled because the primary objective was safety and not efficacy. Observed treatment effects are being further explored in the Phase 2 SPEARHEAD-1 trial. In addition, the study was not powered for either safety or efficacy; hence the data are summarized descriptively.

Recruitment

Patients were recruited from 05July2017 to 11Nov2019 by participating investigators from a screening study initiated to pre-screen patients with advanced solid tumors for the presence of inclusion and exclusion alleles (NCT02636855). A total of 854 HLA-A*02-eligible patients proceeded to tumor MAGE-A4 testing, of which 225 were MAGE-A4 positive. Eligibility criteria included age ≥ 18 to ≤ 75 years, histologically confirmed cancer diagnosis, and measurable disease according to Response Evaluation Criteria in Solid Tumors version 1.1 before lymphodepleting (LD) chemotherapy. No self-selection or other biases are expected as the inclusion and exclusion criteria detail eligibility for enrollment.

Ethics oversight

Patients had voluntarily agreed to participate by giving written informed consent in accordance with International Council on Harmonization (ICH) Good Clinical Practice (GCP) guidelines and applicable local regulations. No compensation was provided for study participation. Participants may have received reimbursement for any costs incurred as a results of study participation.

The final study protocol and subject informed consent documentation was approved by the Institutional Review Board (IRB)/Independent Ethics Committee (IEC) and any other site level committee deemed appropriate by the 10 institutions listed below. Approval from each applicable committee was received in writing before initiation of the study. Below lists the institutional review boards and ethics committees.

Site: Duke University Medical Center

Investigator: Jeffrey Clarke, MD

Institutional review board or ethics committee: Duke University Health System Institutional Review Board, 2424 Erwin Road, Duke University Medical Center, Suite 405, Box 2712, Durham, NC 27705

Chairperson: Jody Power

Site: The University of Texas MD Anderson Cancer Center

Investigator: David S. Hong, MD

Institutional review board or ethics committee: The University of Texas MD Anderson Cancer Center, Institutional Review Board 7007 Bertner Avenue, Unit 1637, Houston, TX 77030

Chairperson: Dr. Jennifer Litton, M.D.

Site: H. Lee Moffitt Cancer Center and Research Institute

Investigator: Mihaela Druta, MD

Institutional review board or ethics committee: Advarra IRB, 6940 Columbia Gateway Drive Suite 110, Columbia MD 21046

Chairperson: Advarra, Tony Davis

Site: Sylvester Comprehensive Cancer Center

Investigator: Brian Matthew Slomovitz, MD

Institutional review board or ethics committee: University of Miami Institutional Review Board, 1400 NW 10th Avenue, Suite 1200A, Miami, FL 33136

Chairperson: Daniel H. Kett

Site: Washington University School of Medicine

Investigator: Brian Van Tine, MD

Institutional review board or ethics committee: Western Institutional Review Board (WIRB), 1019 39th Avenue SE Suite 120, Puyallup, WA 98374

Chairperson: Donald D. Deieso

Site: Princess Margaret Cancer Center
 Investigator: Dr. Marcus Butler
 Institutional review board or ethics committee: University Health Network, Research Ethics Board, 700 University Avenue Hydro Building, 10th Floor Suite 1056 Toronto, Ontario M5D 1Z5
 Chairperson: Dr. David Hogg

Site: James Cancer Hospital and Solove Research Institute
 Investigator: David A. Liebner, MD
 Institutional review board or ethics committee: The Ohio State University Cancer Institutional Review Board Office of Responsible Research Practices, 1960 Kenny Road, 300 OSU Research Foundation, Columbus, OH 43210
 Chairperson: William Carson III, MD

Site: The Sarah Cannon Research Institute
 Investigator: Melissa L. Johnson, MD
 Institutional review board or ethics committee: Western Institutional Review Board, 1019 39th Avenue SE Suite 120, Puyallup, WA 98374
 Chairperson: Donald D. Deieso

Site: Fox Chase Cancer Center
 Investigator: Anthony Olszanski, MD
 Institutional review board or ethics committee: WIRB, 1019 39th Avenue SE Suite 120, Puyallup, WA 98374
 Chairperson: Donald D. Deieso

Site: Roswell Park Cancer Institute
 Investigator: Adekunle Odunsi, MD, PhD
 Institutional review board or ethics committee: Roswell Park Institute Institutional Review Board, Elm & Carlton Streets, Buffalo, New York 14263
 Chairperson: Donald Handley

Note that full information on the approval of the study protocol must also be provided in the manuscript.

Field-specific reporting

Please select the one below that is the best fit for your research. If you are not sure, read the appropriate sections before making your selection.

Life sciences Behavioural & social sciences Ecological, evolutionary & environmental sciences

For a reference copy of the document with all sections, see nature.com/documents/nr-reporting-summary-flat.pdf

Life sciences study design

All studies must disclose on these points even when the disclosure is negative.

Sample size

This is a first-in-human, open-label, single arm, Phase 1, safety and dose finding study. The sample size was based on clinical judgment. The study was not powered for either safety or efficacy and hence the data are summarized descriptively. The study used a modified 3 + 3 cell dose escalation design to evaluate dose-limiting toxicities and determine the target cell dose range. Following the dose escalation phase, up to 30 patients total at the selected dose range (inclusive of patients accrued during the dose escalation) were treated across all the eligible tumor types in the dose expansion phase, to characterize and better assess overall safety and anti-tumor activity. Up to an additional 10 were treated at the selected dose range in a radiation sub-study.

Data exclusions

No data were excluded.

Replication

Replication is not applicable because this is a Phase 1 safety and dose-finding study. However, further assessment of outcomes following intervention with afami-cel is near completion in the Phase 2 SPEARHEAD-1 trial.

Randomization

Randomization is not applicable because this is an open-label, single arm, Phase 1 safety and dose finding study. Covariates were not controlled because the primary objective was safety and not efficacy. In addition, the study was not powered for either safety or efficacy; hence the data are summarized descriptively. Observed treatment effects are being further explored in the Phase 2 SPEARHEAD-1 trial.

Blinding

Blinding is not applicable because this is an open-label, single arm study.

Reporting for specific materials, systems and methods

We require information from authors about some types of materials, experimental systems and methods used in many studies. Here, indicate whether each material, system or method listed is relevant to your study. If you are not sure if a list item applies to your research, read the appropriate section before selecting a response.

Materials & experimental systems

n/a	Involved in the study
<input type="checkbox"/>	<input checked="" type="checkbox"/> Antibodies
<input checked="" type="checkbox"/>	<input type="checkbox"/> Eukaryotic cell lines
<input checked="" type="checkbox"/>	<input type="checkbox"/> Palaeontology and archaeology
<input checked="" type="checkbox"/>	<input type="checkbox"/> Animals and other organisms
<input type="checkbox"/>	<input checked="" type="checkbox"/> Clinical data
<input checked="" type="checkbox"/>	<input type="checkbox"/> Dual use research of concern

Methods

n/a	Involved in the study
<input checked="" type="checkbox"/>	<input type="checkbox"/> ChIP-seq
<input type="checkbox"/>	<input checked="" type="checkbox"/> Flow cytometry
<input checked="" type="checkbox"/>	<input type="checkbox"/> MRI-based neuroimaging

Antibodies

Antibodies used

Reagent; Clone; Supplier Titer (μ l); Dilution:

- 1) Live/Dead Aqua; Fisher Scientific; 0.25; 200
- 2) CD3 BUV395; SK7; BD Biosciences; 0.50; 100
- 3) CD4 BUV496; SK3; BD Biosciences; 0.50; 100
- 4) CD8 BUV737; SK1 BD Biosciences; 1.00; 50
- 5) CD45RA APC-Cy7; HI100 Biolegend; 0.25; 200
- 6) CD197 (CCR7) PE-Cy7; G043H7; Biolegend; 1.00; 50
- 7) Dextramer PE:MAGE A-4; Immudex; 10.0; 5

Validation

All antibodies are validated for specificity to their respective target on human cells as detailed by the manufacturers.

Clinical data

Policy information about [clinical studies](#)All manuscripts should comply with the ICMJE [guidelines for publication of clinical research](#) and a completed [CONSORT checklist](#) must be included with all submissions.Clinical trial registration [NCT03132922](#)Study protocol [Provided with the submission but not to be published.](#)Data collection [Data were collected at medical centers and hospitals at 10 sites across North America \(USA, 9 sites, 28 patients; Canada, 1 site, 10 patients\). Recruitment took place between 05July2017 and 11Nov2019, and data were collected until 01Sept2020.](#)

Investigator; Location; Number of Patients Treated

David S Hong, MD; The University of Texas MD Anderson Cancer Center, Houston, TX; 16

Marcus Butler, MD; Princess Margaret Cancer Centre, Toronto, ON, Canada; 10

Brian Van Tine, MD; Washington University School of Medicine, St. Louis, MO; 7

Anthony Olszanski, MD; Fox Chase Cancer Center, Philadelphia, PA; 2

David A Liebner, MD; James Cancer Hospital and Solove Research Institute, Columbus, OH; 1

Melissa L Johnson, MD; The Sarah Cannon Research Institute, Nashville, TN; 1

Adekunle Odunsi, MD, PhD; Roswell Park Cancer Institute, Buffalo, NY; 1

Jeffrey Clarke, MD; Duke University Medical Cancer Center, Durham, NC; 0

Mihaela Druta, MD; H. Lee Moffitt Cancer and Research Institute, Tampa, FL; 0

Brian M Slomovitz, MD; Sylvester Comprehensive Cancer Center, Miami, FL; 0

Outcomes

[The primary objective was evaluation of safety and tolerability with endpoints including TEAEs, serious adverse events \(SAE\), DLTs, and detection of replication competent lentivirus \(RCL\). Secondary endpoints included overall response rate \(ORR\) confirmed by RECIST v1.1, best overall response \(BoR\), time to response \(TTR\), duration of response \(DoR\), duration of stable disease \(DoS\), progression-free survival \(PFS\), and overall survival \(OS\). Exploratory objectives included evaluation of cell persistence and cytokines.](#)

Flow Cytometry

Plots

Confirm that:

- The axis labels state the marker and fluorochrome used (e.g. CD4-FITC).
- The axis scales are clearly visible. Include numbers along axes only for bottom left plot of group (a 'group' is an analysis of identical markers).
- All plots are contour plots with outliers or pseudocolor plots.
- A numerical value for number of cells or percentage (with statistics) is provided.

Methodology

Sample preparation

Cryopreserved manufactured product (MP) and peripheral blood mononuclear cells (PBMC) from human clinical trial subjects were thawed, stained and washed for immunophenotypic profiling using multicolor staining panels (CD3 (SK7), CD4 (SK3), CD8 (SK1), BD Biosciences, Franklin Lakes, NJ, USA; CD45RA (H1100), CCR7 (G043H7), Biolegend, San Diego, CA, USA; Live/Dead Fix Aqua, Fisher Scientific, Waltham, MA, USA). For all samples, in the CD3+ live population, subsets of CD4+ and CD8+ cells (assessed for transduction using an MHC dextramer reagent) were further classified into memory subtypes by expression of CCR7 and CD45RA.

Instrument

BD LSR Fortessa

Software

FlowJo

Cell population abundance

No sorting was performed

Gating strategy

FSC/SSC gating on lymphocytes, viability dye dead cell exclusion gate and gates for all single markers were set in relation to FMO (fluorescence minus one) controls

- Tick this box to confirm that a figure exemplifying the gating strategy is provided in the Supplementary Information.